

Sudan University of Sciences and Technology

Collage of Graduate Studies

**Morphometric Analysis of Internal Auditory canal in
Sudanese Population using Computed Tomography**

تحليل القياسات الشكلية للقناة السمعية الداخلية لدى السودانيين باستخدام الأشعة المقطعية

**A Thesis Submitted of Partial Fulfillment for the Requirement of M.SC.
Degree in Diagnostic Radiological Technology**

By:

Malaz Mohammed Mustafa Mohammed

Supervisor:

Dr. Hussien Ahmed Hassan

2020

Chapter one

Introduction

Chapter Two

Literature review

Chapter Three

Materials and Methods

Chapter Four

Results

Chapter Five

Discussion, Conclusion and
Recommendations

References

Appendices

الآية

قال تعالى:

﴿الرُّسُلَ السَّمْعَ وَ الْبَصَرَ وَالْفُؤَادَ كُلُّ أُوْنَيْكَ كَانَ عَنْهُ مَسْئُولًا﴾

صدق الله العظيم

(سورة الاسراء ﴿ الآية (36) ﴾

DEDICATION

TO MY PARENTS

TO MY BROTHERS

TO MY SISTERS

TO MY TEACHERS, FRIENDS AND COLLEAGUES

ACKNOWLEDGEMENT

I am grateful to Allah, without His support I would have never been able to accomplish this study.

Special thanks to my supervisor Dr. Hussien who was abundantly helpful and offered invaluable assistance, support and guidance.

A special thanks and respect to all teachers in the college.

ABSTRACT

This study was aimed to study and analysis the morphological changes and diameters of the internal auditory canal by using computed

Data was obtained retrospectively from 80 patients of different ages and gender .

The study was done at Modern Medical Center (MMC) during 2019 year.

CT images were obtained by taking 2mm sections using ultra high algorithm in axial planes. The results were then analyzed statistically.

In this study

CT has major role in the demonstration of detailed anatomy and identifying various findings related to the location, extent and shape change of the canal which a great importance in guiding the surgical approach that can prevent further serious complication

ملخص الدراسة

هدفت هذه الدراسة لدراسة و تحليل التغيير في الشكل و اختلاف الابعاد للقناة السمعيه الداخليه بواسطة الاشعة المقطعية .

وقد اشتملت الدراسة علي 80 مريض من مختلف الاعداد والجناس .

اجريت هذه الدراسة خلال عام 2019 في المركز الطبي الحديث .

تم اجراء الأشعة المقطعية لجميع الحالات في الوضع المحوري عن طريق اخذ مقاطع متجاوره ,سمك المقطع 2ملم مع استخدام مرشح عالي التمييز وقد استخدم وسيط التباين حسب الحاجة وتم تحليل النتائج احصائيا .

أكدت الدراسة ان للأشعة المقطعية دورا اساسيا في المقدرة عن الكشف عن الاختلافات التشريحية الطبيعية للقناة السمعية التي تمثل اهمية قصوي لجراحي الانف والاذن والحنجره و الاعصاب مما يفيد في اختيار الاسلوب المناسب للمريض وعدم تعرضه لمخاطر ومضاعفات , و قياس ابعاد القناة بدقة عالية , كما يمكنها الكشف عن التغيرات الطارئة علي العظم.

TABLE OF CONTENTS

الآية.....	I
DEDICATION.....	II
ACKNOWLEDGEMENTS.....	III
ABSTRACT.....	IV
Arabic Abstract.....	V
TABLE OF CONTENTS	VI
LIST OF TABLES.....	IX
LIST OF FIGURES	X
LIST OF ABBREVIATIONS	XI

Chapter One

Introduction

1. Introduction.....	1
1.2.Problem of the study:.....	2
1.3. Objectives:	2
1.3.1. General objective	2
1.3.2. Specific objectives.....	2
1.4 overview of the Thesis:-.....	3

Chapter Two

Literature Review

2.Literature Review	4
2.1: Anatomy of the temporal bone :	4

2.2: Anatomy of the ear and hearing process :.....	4
2.2.1: anatomy of the external ear :	5
2.2.2 anatomy of the middle ear :	5
2.2.3 anatomy of the inner ear :	5
2.2.4 the vestibular and cochlear aqueduct :	7
2.3 the internal auditory meatus :	7
2.3.1 structure of the IAM :	7
2.3.2 physiology of the IAM:	8
2.3.3 blood supply of the IAM.....	9
2.4: cranial nerves :	9
2.5:the cerebellopontine angle cistern	9
2.6pathology of the IAM and the CPA:	10
2.6.1 acoustic neuroma :	10
2.6.2 meningioma :	10
2.6.3 cavernous hemangioma :.....	11
2.6.4 neurofibromatosis :.....	11
2.7 IAM imaging :.....	11
2.7.1 MRI imaging :	12
2.7.2 CT imaging :	12
2.8 previous studies :	12
2.9 CT instruments and techniques :.....	12

Chapter Three

Materials and Methods

3.1subjects :	26
3.1.1 Inclusion criteria	26

3.1.2 Exclusions criteria	26
3.2 data collection :	26
3.4 technique protocols :.....	26

Chapter Four

Data analysis and result

4.1 Result	29
------------------	----

Chapter Five

Discussion, Conclusion and Recommendations

5.1 Discussion.....	37
5.2 Conclusion:	39
5.3 Recommendations:	40
References:.....	41
Appendixes	36

LIST OF TABLELIST OF TABLES

Table	Table names	Page.
(4-1)	frequency distribution of gender	31
(4-2)	frequency distribution of age \years	32
(4-3)	descriptive statistic of age \years and measurements (min, max, mean± Std. Deviation)	33
(4-4)	frequency distribution of shape	33
(4-5)	correlation between age and measurements of right internal auditory canal	34
(4-6)	correlation between age and measurements of left internal auditory canal	34
(4-7) a	compares mean measurements of internal auditory canal in different gender	35
(4-7) b	t. test for compare mean measurements of internal auditory canal in different gender	36
(4-8)	compare mean measurements of internal auditory canal in different age group	37
(4-9) a	compares mean measurements of	40

	internal auditory canal in different in the children and adult	
(4-9) b	t. test for compare mean measurements of internal auditory canal in children and adult	41
(4-10)	correlation between right and left sides of internal auditory canal	42

LIST OF FIGURES

Fig	Figure names	Page No.
(2- 1)	Diagram of the ear	4
(2-2)	Schematic arrangement of the particular area of the IAM	8
(2- 3)	Cadaveric picture of the IAM	9
(2- 4)	Diagram of the blood supply of the inner ear and IAM	10
(2- 5)	Diagram of the cranial nerve	17
(2-6)	Diagram of the facial nerve and VCN inside IAM	18
(2-7)	Diagram of MRI imaging axial T2 section at the level of IAM	22
(2-8)	CT imaging of the IAM	23
(2-9)	CT spiral principle	26
(2-10)	Lateral scout determination of the start and end scan level of IAM	27
(4-1)	frequency distribution of gender	31
(4-2)	frequency distribution of age \years	32
(4-3)	frequency distribution of shape	33
(4-4)	scatterplot shows relationship between age and opening width	37
(4-5)	scatterplot shows relationship between age and length	38
(4-6)	scatterplot shows relationship between age and AP	38

(4-7)	scatterplot shows relationship between age and area	39
(4-8)	scatterplot shows relationship between age and IAC\VA	39

List of abbreviations

ACA	Anterior Cerebral Artery
AICA	Anterior Inferior Cerebral Artery
AP	Anteroposterior
AN	Acoustic neuroma
CPA	Cerebropontine angle
CSF	CerebroSpinal Fluid
CT	Computed Tomography
CSF	Cerebro spinal fluid
MCA	Medial Cerebral Artery
MRI	Magnetic Resonance Imaging
NF	NeuroFibromatosis
IAC	Internal Acoustic Canal
IAM	Internal Auditory Canal

Chapter One

Introduction

1.1 Introduction

The internal acoustic canal (IAC), also known as the internal auditory canal or meatus (IAM), is a bony canal within the petrous portion of the temporal bone that transmits nerves and vessels from within the posterior cranial fossa to the auditory and vestibular apparatus. Quantitative and morphometric assessment of the internal auditory canal (IAC) are essential to establish the anatomical bases for microsurgery of the cerebellopontine angle and acoustic neuroma, which may produce bone changes and is an important intracranial pathology (Barreto-1993). Many clinical and experimental studies have been done to analyze the anatomical and functional aspects of the IAC in human beings; however, with the advance of new diagnostic techniques in the area of otology, studies of the human temporal bone are being redone to provide better anatomical knowledge for surgeons, since there are great inter individual variability and structural variations that may occur regarding the other adjacent structures. These studies will hopefully avoid misinterpretations and improve the quality of radiological results (Chakeres-1984). It is essential to know the temporal bone well since it is very complex. Each one of its structures develops differently and they are all very close to each other. According to the literature, the IAC is accessed via the middle cranial fossa. The IAC is a narrow canal that extends for roughly 1cm within the petrous part of the temporal bone and has the shape of an oval foramen. The IAC is closed laterally by a thin and perforated sheet of bone that separates it from the inner ear. It is through this plane that the blood vessels, the facial nerve and the vestibulocochlear nerve pass. This nerve divides into two near the lateral extremity of the internal acoustic meatus, forming the cochlear nerve and the vestibular nerve (Pellet-1990).

Since previous reports indicate variation in the anteroposterior (AP) diameter and length of the canal, in order to avoid damages to the labyrinth, a preview of the measurements of the IAC is important for interpreting radiographs (Fujita-1994). Variations between

the left and right sides are also very common. The canal is considered stenotic if its diameter is smaller than 2 mm. The normal diameter varies from 4 to 8 mm (GUIRADO-1992). There are many publications that describe how the shape, size and position of the human IAC can influence certain inner ear disorders. The IAC may serve as a canal for inner ear infection spreading that could damage it or reach the central auditory pathways (Paparella-1993). There are many techniques that can be used to determine the location of the IAC. Among them high resolution CT is a sensitive method for the detection of anomalies that allows the correlation between radiological images and clinical data. This canal is better seen in axial views (Virapongse -1982).

1.2 Problems of the study:

There is anatomical variations in shape and diameter of internal auditory canals between people, knowledge of these variation is crucial in surgical planning and interventional examination.

1.3 Objectives

1.3.1 General objectives

To determine to the morphometric variations of internal auditory canal by computed tomography imaging.

1.3.2 Specific objectives

- To characterize the morphology morphology of the (IAC) in children and adults.
- To analyze the dimensions of internal auditory canals, which will be determined by measuring the nearby areas and structures using a system of digital image processing.

1.5 Overview of the thesis:

Chapter one including introduction, objectives, problems of the study, methodology of the research. Chapter two contain literature review , chapter three contain material and methods, chapter four contain the results and chapter five contain discussion, conclusion and recommendations then appendix and references.

Chapter Two

Literature Review

2-1 The Temporal bone:

The temporal bones contain the sensory organ of hearing and balance. it is consist of five portion : the squamous , the tympanic , the mastoid ,the zygomatic , and petrous segment which contributes to form the cranial vault. It contains portions of the carotid artery and jugular venous drainage system, and is intimately related to the Dura of the middle and posterior fossa. (Karthikeyan 2007).

Anteriorly, the squamous extend to form zygomatic arch and by articular tubercle form anterior boundary of mandibular fossa which depresses these particular with condyle of mandible to great tempromandibular joint. The tympanic portion lies forms the majority of the external auditory meatus.

The mastoid antrum is an air-filled cavity that communicates with the middle ear (tympanic cavity).

The petrous portion of the temporal bone contributes to form both the middle cranial fossa with the greater wing and body of the sphenoid bone and the posterior cranial fossa with the occipital bone .At the surface is the opening to the internal auditory canal, Other openings associated with the posterior surface of the petrous pyramid are the jugular foramen and the carotid canal,which provide passage for the internal jugular vein and the internal carotid artery.. Between the apex of the petrous pyramid, The body of the sphenoid bone and the basilar portion of the occipital bone is jagged slit termed the foramen lacerum, which contains cartilage and allows the internal carotid artery to enter the cranium, providing small arteries that supply the inner surface of the cranium .the inferior surface of the petrous pyramid gives rise to the long slender styloid process that is attached to several muscles of the tongue and ligament of the hyoid bone. The interior of the petrous pyramid houses the delicate middle and inner ear structure. Figure (2.1). (Frank, 1990) (Lorrie, 2007).

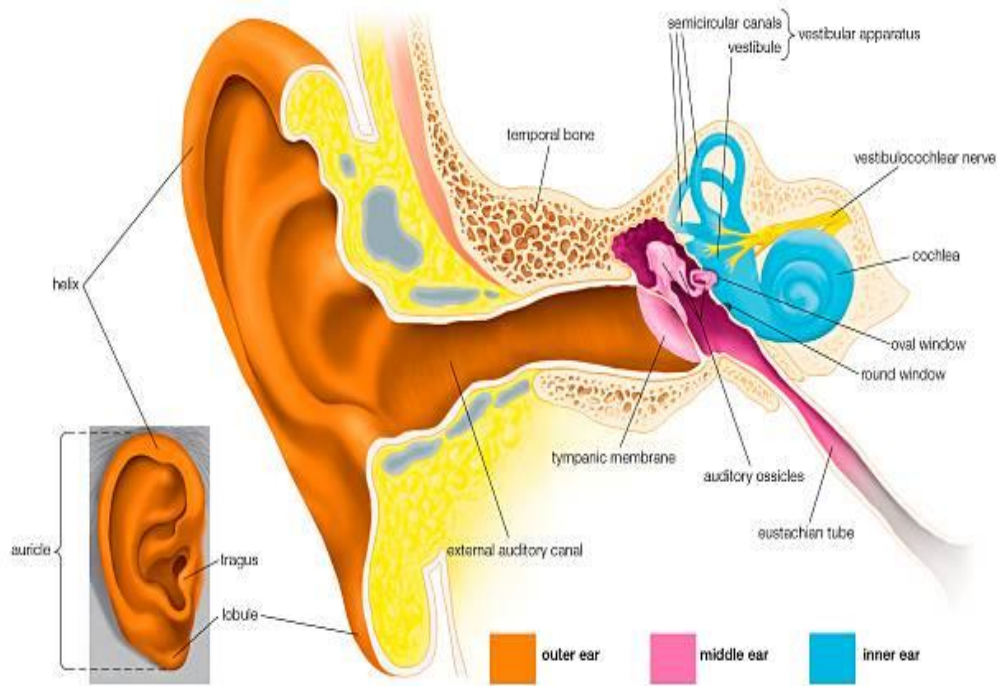


Figure (2. 1): Overview diagram of the ear. This illustration represents the outer ear (pinna, external auditory canal, and outer portion of the tympanic cavity known as the ear drum), the middle ear (malleus, incus, stapes, and Eustachian tube) and the inner ear (cochlea, semicircular canals, and the vestibule). (Hallowell, 1970).

2-2 Anatomy of The Ear and hearing process:

2-2-1 The external ear:

The external ear consists of the pinna and the external auditory meatus. The external meatus is 3.5 cm long and runs medially to the ear drum or tympanic membrane. The outer part of the canal is cartilaginous and the medial two thirds are bony. The entire canal is lined by skin. (Stephanie, 2004).

2-2-2 The middle ear:

The middle ear is a slit-like cavity housed in the petrous bone. It lies between the tympanic membrane laterally and the inner ear medially. It has an upper part, which is recessed superiorly into the petrous bone and is known as the epitympanic recess or attic, as it lies at a higher level than the tympanic membrane. The roof of the cavity is formed by a thin layer of bone called the tegmen tympani, separating it from the middle cranial fossa and temporal lobe of the brain. The attic communicates with the mastoid air cells

through a narrow posterior opening called the aditus and antrum. This is important, as infection may spread from the middle ear to the mastoid air cells, which are related posteriorly to the sigmoid sinus and cerebellum in the posterior cranial fossa. A tiny spur of bone, the scutum, separates the external auditory canal and the antrum, where the tympanic membrane is attached. The presence or erosion of the scutum is a sensitive marker for erosion by middle-ear disease states, including cholesteatoma. The lower part of the middle ear contains the ossicles, and is continuous inferiorly with the eustachian tube, which opens into the lateral wall of the nasopharynx. This tube is 3.5 cm long, bony at first, and cartilaginous in its lower portion. The floor of the middle ear is a thin plate of bone separating the cavity from the bulb of the jugular vein.

The lateral wall of the cavity is the tympanic membrane and the ring of bone to which it is attached. The medial wall of the middle ear also forms the lateral wall of the inner ear, and its middle-ear surface is shaped by the contents of the inner ear. The lateral semicircular canal causes a prominence in the wall superiorly. Below this is a bulge caused by the cochlea called the promontory.

The ossicles from lateral to medial, these are the malleus, the incus, and the stapes. The handle and lateral process of the malleus is attached to the tympanic membrane and can be easily seen on physical exam. The long process of the incus can often be seen through the posterior superior quadrant of the membrane. The stapes is attached to a footplate which is in direct contact with the fluid of the inner ear. (Frank, 1990) (Stephanie, 2004).

2-2-3 The inner ear:

Consists of a fluid-filled labyrinth which functions to convert mechanical energy into neural impulses. The bony labyrinth is subdivided into smaller compartments by the membranous labyrinth. Fluid surrounding the membranous labyrinth is called perilymph; fluid within is called endolymph. There are three main divisions of the bony labyrinth:

- **Vestibule**—Just medial to the oval window, and contains the utricle and the saccule, two organs of balance. The vestibule is an antechamber, leading to both the cochlear and the semicircular canal.
- **The cochlea**—A snail-shaped chamber anterior to the vestibule. It bulges into the middle ear and its bony covering is the *promontory*. The cochlea also communicates with the middle ear via the round window. In this organ, sound waves are converted into neural impulses with elaborate coding.
- **The Semicircular canals**—Three in number; project posteriorly from the vestibule. These organs detect angular acceleration. They consist of a superior, posterior and lateral, or horizontal canals.

The nerve fibers from the labyrinth make up the auditory nerve which consists of a cochlear nerve and a superior and inferior vestibular with both afferent and efferent fibers from the respective sensory end organs. This nerve enters the cranial cavity via the internal auditory canal. (Stephanie, 2004). (Karthikeyan 2007).

2-2-4The vestibular and cochlear aqueducts:

The cochlea is situated anteroinferiorly to the vestibule and resembles a snail shell with two and three quarter turns the cochlear aqueduct runs medial to lateral from the basal turn of the cochlea to the lateral border of the jugular foramen.

Vestibule aqueduct is narrow bony canal that runs through the skull, connected the inner ear (vestibule) to the cranial cavity.

Running through this bony canal is a membranous (tube) called endolymphatic duct fill with fluid called endolymph. This duct through the bony vestibular aqueduct and dumps into the endolymphatic sac which lies between the inside of the skull and the membranes that cover the brain.

Endolymph normally flows away from the organ of the inner ear and toward the endolymphatic sac. In LVAS the endolymphatic duct and sac are much large than normal. This enlarge size allow the endolymph to flow from the endolymphatic sac back into the hearing and balance organ. (Karthikeyan 2007).

2-3 The internal auditory meatus:

Internal auditory canal (meatus acusticus internus) is a canal within the petrous part of temporal bone of the skull between the posterior cranial fossa and the inner ear. (Gray 1918).

2-3-1 structure:

The opening to the meatus is called the porus acusticus internus or internal acoustic opening. It is located inside the posterior fossa of the skull, near the center of the posterior surface of the petrous part of the temporal bone. Its outer margins are smooth and rounded. The canal which comprises the internal auditory meatus is short (about 1 cm) and runs laterally into the bone.

The lateral (outer) aspect of the canal is known as the fundus which is located inside the pyramid of the temporal bone. The fundus is subdivided by two thin crests: the falciform and the bills bar crest.

From medial to lateral, the transverse (falciform) crest first divides the meatus into superior and inferior sections. The upper compartment contains the facial nerve (situated anteriorly) and the superior vestibular branch of the eighth cranial nerve (situated posteriorly), and the lower compartment contains the acoustic (situated anteriorly) and inferior vestibular branches of the eighth cranial nerve (situated posteriorly) and the singular foramen (situated postero-inferiorly).

A second vertical crest (bills bar) then divides the upper passage into anterior and posterior sections.

Accordingly, the fundus is conceptually divided more commonly into four quadrant areas according to the four major nerve branches of the inner ear:

Anterior superior: facial nerve area (contains facial nerve and nervus intermedius).

Anterior inferior: cochlear nerve area (contains cochlear nerve).

Posterior superior: superior vestibular area (contains superior division of vestibular nerve).

Posterior inferior: inferior vestibular area (contain inferior deviation of vestibular nerve)
(figure 2-2) (gray 1918).

2-3-2 Function:

The IAM as important passage of many nerves and vessels , it contain : facial nerve, Vestibular ganglion, Vestibulocochlear nerve(which divides near the lateral end of IAM into a two parts: a cochlear nerve and vestibular nerve), Labyrinthine artery (usually branches of the AICA or basilar artery), Nerves intermedius (sensory component of CN VII), Facial motor root (motor component of CN VII), Cochlear nerve (component of CN VII), Superior vestibular nerve (component of CN VII).(figure 2-3).

The first part of the facial nerve runs in the internal auditory meatus. The second part runs anteriorly from this in its bony canal, then curves laterally and posteriorly around the cochlea to the anterior part of the medial wall of the middle-ear cavity. This U-bend around the cochlea is known as the genu of the nerve.

Superior vestibular area is a place of transition of the utriculoampullary nerve which originates from junction of the utricular nerve, anterior and lateral ampullar nerve.

(Agirdir, 2004) (. Brunsteins 1995).

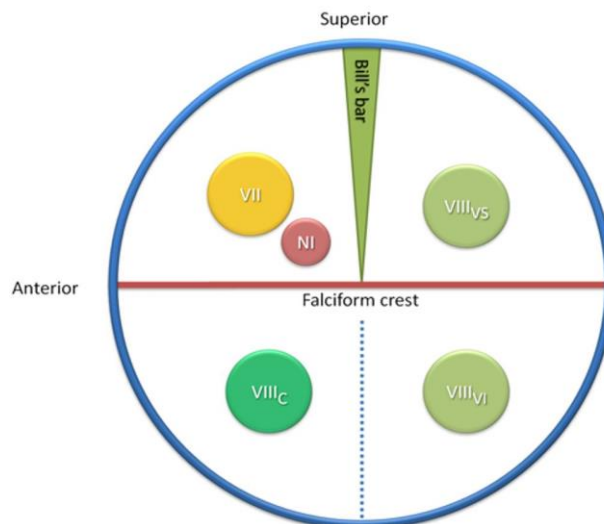


Figure (2.2): schematic arrangement of the particular area of the IAM VII facial nerve NI nervus intermedius VIIIvs superior divition of the vestibular nerve VIIIc cochlear nerve VIIIvi inferior divition of vestibular nerve

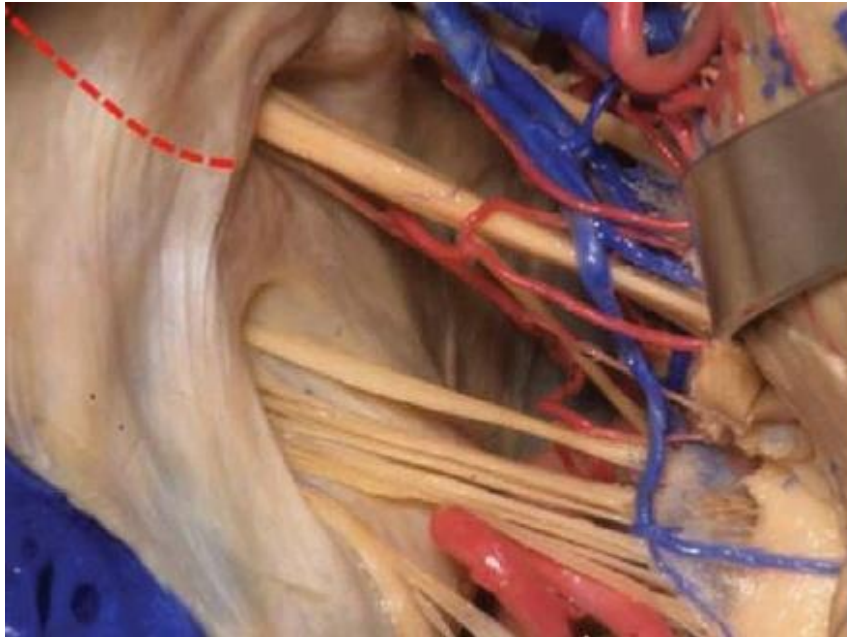


Figure (2. 3): cadaveric picture of IAM

2-3-3 Blood supply of the IAM:

Brain supply by two source:

- Internal carotid artery.
- Basilar artery.

The internal carotid artery is subdivided to the Anterior and middle cerebral arteries.

Then the anterior cerebral artery ACA branches to:

Cortical branches; for medial surface back to the parietooccipital fissure

Central branches: to the anterior part of corpus striatum and part of anterior limb of internal capsule

Septal branches: for septum lucidum

Collasal branches: for corpus callosum except the splenium

And medial cerebral artery MCA branches to:

Internal capsule and corpus striatum

The basilar vertebral artery divided to two posterior cerebral arteries PCA and its branches is:

Anterior inferior cerebral arteries

Internal auditory arteries

Pontine branches

Superior cerebral arteries. Figure (2. 4).

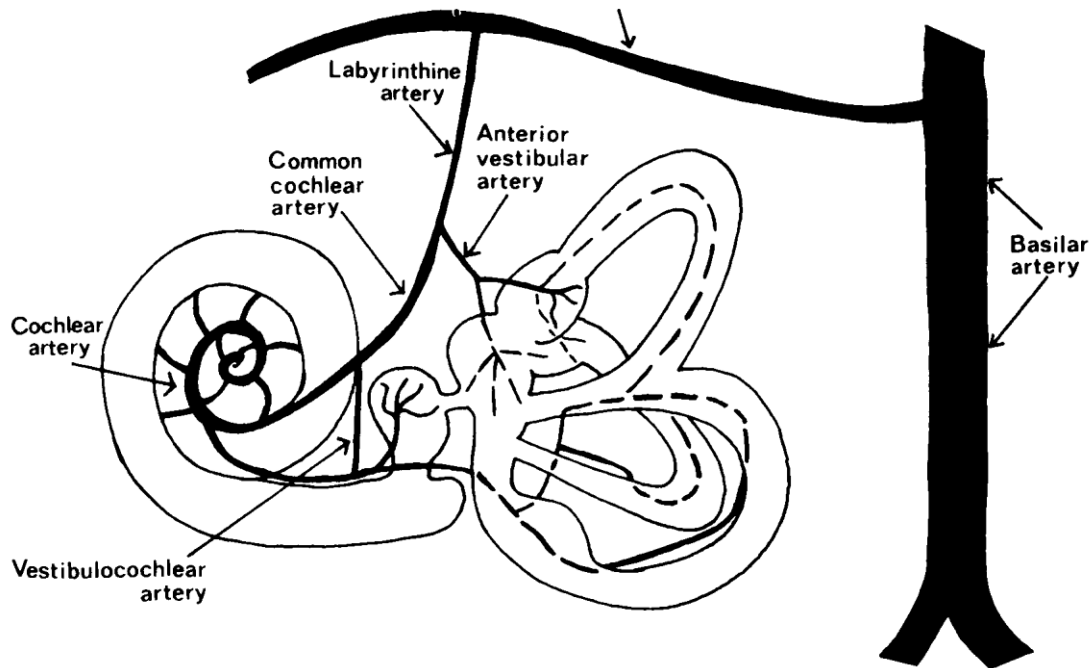


Figure (2. 4): Overview diagram of blood supply of inner ear and internal auditory canal. (Merchant, 2010).

2-4 cranial nerves: Figure (2. 5):

2-4-1 Vestibulocochlear Nerve (CN VIII):

Function:

The vestibulocochlear nerve is the sensory nerve for hearing (cochlear) and equilibration (vestibular).

Anatomy:

Hearing depends on transduction of mechanical stimuli to elicit an electrical response in hairy cells in the organ of Corti, which respond to specific stimulus frequencies. This is possible because of the amplification of sound waves by the tympanic membrane and

middle ear bones, and by the oval window and basilar membrane on the inner ear. The organ of Corti has hair cells with villi that permit transduction of mechanical stimuli to electrical activity, which is then conducted by spiral ganglion neurons to the brain stem. Vestibular input originates from hair cells stimulation of gelatinous material embedded with otoconias (calcium carbonate stones) on the vestibular labyrinth. This organ can measure linear and angular acceleration. Linear acceleration is detected by the utricle and the saccule; angular accelerations are measured by the semicircular canals. These stimuli are conducted by Scarpa ganglion neurons to originate the vestibular division of the eighth nerve. From here, central processes pass the cochlear nerve to the cochlear and vestibular nuclei (Monkhouse, 2006). CN VIII passes across the internal auditory canal and divides into three branches: the cochlear nerve, which passes medially and inferiorly; the superior vestibular nerve, which passes laterally and superiorly; and the inferior vestibular nerve, which passes inferiorly and laterally to the vertical and horizontal crests of the IAC (Agur & Dalley, 2013). The nerve then passes to the subarachnoid space at the cerebellopontine cistern, lateral to the facial nerve, and in relation to the meatal and postmeatal segment of the AICA. It runs in a medial and posterior direction to reach the cerebellopontine angle of the brain stem, crossing the pontomedullary sulcus (Rhoton, 2000a). The cochlear nerve reaches the cochlear nuclei laterally in the floor of the fourth ventricle, the sensory neurons of which form the lateral lemniscus tract to inferior colliculi, dorsally in the midbrain. From here, the tract continues to the medial geniculate bodies in the posterior and medial part of the thalamus. These nuclei form the auditory radiation fibers in the sublentiform section of the internal capsule, reaching Heschl's gyri at the opercular surface of the temporal lobe (Wen et al., 1999). The vestibular nerve reaches the vestibular nuclei in the floor of the fourth ventricle; vestibular impulses pass to the floccular nodule, uvula, and fastigial nucleus of the cerebellum, crossing through the inferior cerebellar peduncle. The vestibular nuclei also project to the spinal cord (vestibulospinal tract), the eye muscle nuclei (medial longitudinal fasciculus), and the ventral posterior nucleus of the thalamus. The vestibular system originates reflexes that stabilize the eyes and body when the head

moves; and vestibulo-ocular reflexes that compensate orbits position for head movements.

Anatomical Landmarks:

- Cochlea and vestibule.
- Inner ear.
- IAC.
- Cerebellopontine angle.
- AICA.
- Lateral part of floor of fourth ventricle. **Figure (2.6):**

2-4-2 Olfactory Nerve (CN I):

Function:

The primary function of the olfactory nerve is to transmit olfactory impulses from the olfactory epithelium of the nose to the brain; it is better referred to as the olfactory bulb and tract and is an outgrowth of the forebrain. The primary sensory neurons are bipolar and are confined to the olfactory epithelium (Binder et al., 2010).

Anatomical Landmarks:

- Cribriform plate.
- Basal surface of frontal lobes.
- Anterior perforate substance.
- Uncus of temporal lobes.

2-4-3 Optic Nerve (CN II):

Function:

The optic pathway transmits visual impulses from the retina to the brain. The optic pathway between the eyeball and the optic chiasm is erroneously called the optic nerve, but it is also an overgrowth of thalamic structures. The primary sensory neurons are bipolar and are confined to the sensitive epithelium of the retina (Dacey, 1996); the optic pathway originates in secondary sensory neurons, also located in the retina.

Anatomical Landmarks:

- Eyeball.
- Optic canal.
- Anterior clinoid process.
- Internal carotid artery.
- Floor of the third ventricle and pituitary stalk.
- Pituitary gland, sella turcica, sphenoidal sinus.
- Cerebral peduncles.
- Temporal horn of lateral ventricle.
- Calcarine sulcus.

2-4-4 Oculomotor Nerve (CN III):

Function:

The third cranial nerve has two main functions: (1) it innervates the extraocular muscles through somatic efferent pathways (except the superior oblique and lateral rectus muscles), being the final pathway of the complex mechanisms controlling ocular movements; and (2) it innervates the constrictor pupillae and ciliary muscles through parasympathetic components, causing constriction of the pupillae by luminous and accommodation stimuli, and the accommodation reflex of the ocular lens.

Anatomical Landmarks

- Orbit.
- Superior orbital fissure.
- Cavernous sinus.
- Interpeduncular fossa.
- Mesencephalon between substantia nigra and tectum.

2-4-5 Trochlear Optic Nerve (CN IV):

Function:

This nerve controls the superior oblique muscle contraction, which rotates the eyeball internally in abduction and lowers the eyeball in adduction.

Anatomical Landmarks:

- Orbit.
- Superior orbital fissure.
- Tentorial incisura.
- Inferior midbrain colliculus.

2-4-6 Trigeminal Nerve (CN V):

Function:

The fifth cranial nerve transmits sensations from the skin of the anterior part of the head, the nasal and oral cavities, teeth, and meninges. It also carries motor fibers to the masticatory muscles.

Anatomical Landmarks:

- Pons.
- Middle cerebellar peduncle.
- Cerebellopontine angle.
- Petrous bone.
- Great wing sphenoid.
- Orbit.
- Infratemporal fossa.

2-4-7 Abducens Nerve (CN VI):

Function:

This nerve supplies the lateral rectus muscle, which abducts the eyeball.

Anatomical Landmarks:

- Fourth ventricle.
- Middle clivus.
- Cavernous sinus and cavernous segment of internal carotid artery.
- Superior orbital fissure.

2-4-8 Facial Nerve (CN VII):

Function:

The main function of the facial nerve is to supply the muscles of facial expression. Its other functions are to conduct taste sensation from the anterior tongue and oral cavity and to effect parasympathetic secretion from the salivary, lacrimal, nasal, and palatine glands (Zhang et al., 2013).

Anatomical Landmarks:

- Middle cerebellar peduncle.
- Internal auditory canal.
- Anteroinferior cerebellar artery.
- Cochlea and semicircular canals.
- Tympanic cavity.
- Mastoid.
- Styloid process.
- Parotid gland.

2-4-9 Glossopharyngeal Nerve (CN IX):

Function:

The main function of the glossopharyngeal nerve is in the gag reflex, because it provides the sensory supply from the oropharynx and posterior part of the tongue.

Anatomical Landmarks:

- Fourth ventricle floor.
- Medullary olive.
- Jugular foramen.
- Internal carotid artery.
- Pharynx.

2-4-10 Vagus Nerve (CN X):

Function:

The main functions of the vagus nerve are phonation and swallowing. It also transmits cutaneous sensory fibers from the posterior part of the external auditory meatus, tympanic membrane, and hypopharynx. It supplies the gut tube as far as the splenic flexure of the transverse colon, and the heart, tracheobronchial tree, and abdominal viscera (Krahl & Clark, 2012).

Anatomical Landmarks:

- Fourth ventricle floor.
- Medullary olive.
- Jugular foramen.
- Internal carotid artery.
- Internal jugular vein.
- Trachea.
- Esophagus.

2-4-11 Accessory Nerve (CN XI):

Function:

The accessory nerve has two parts: cranial and spinal. The cranial part joins the vagus, from which it is functionally indistinguishable, innervating muscles of the larynx and pharynx. The spinal part is motor to the sternocleidomastoid and trapezius muscles and is not really a cranial nerve.

Anatomical Landmarks:

- Medulla.
- Foramen magnum.
- Jugular orifice.
- Posterior cervical triangle.

2-4-12 Hypoglossal Nerve (CN XII):

Function:

This nerve supplies the muscles of the tongue, which are important in chewing, in the initial stages of swallowing, and in speech.

Anatomical Landmarks:

- Fourth ventricle floor.
- Medulla pyramid.
- Occipital condyles.
- External carotid artery.
- Suprahyoid cervical region.

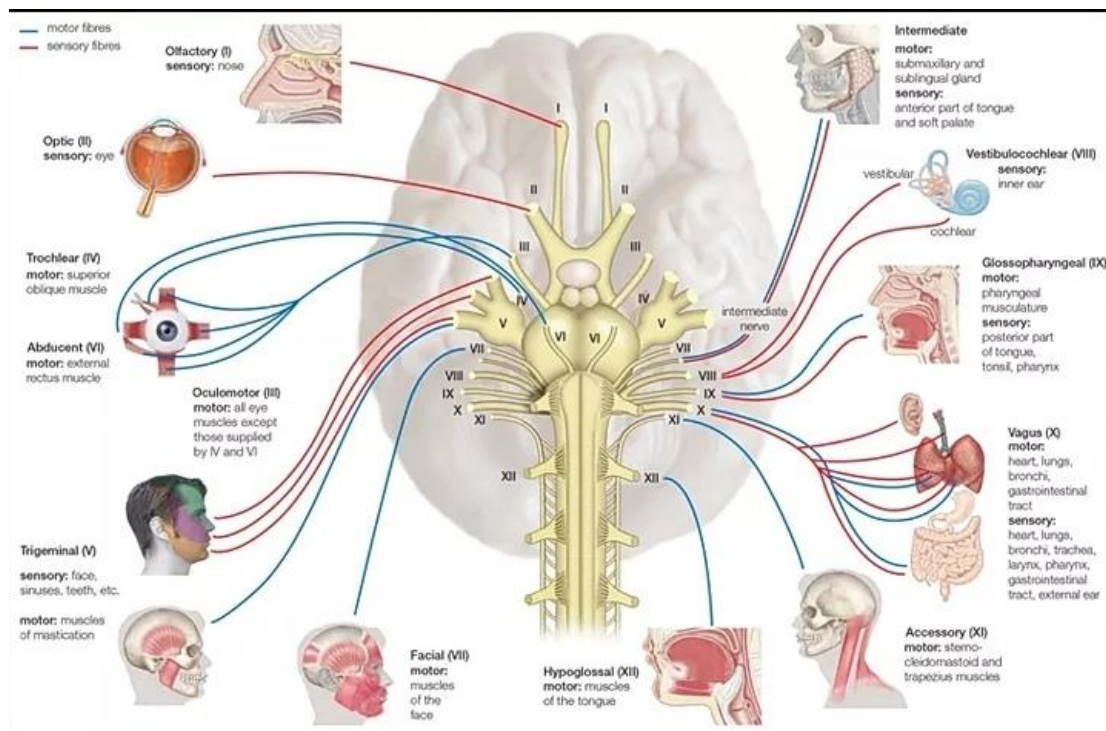


Figure (2.5): Overview diagram of the cranial nerves (merchant, 2010).

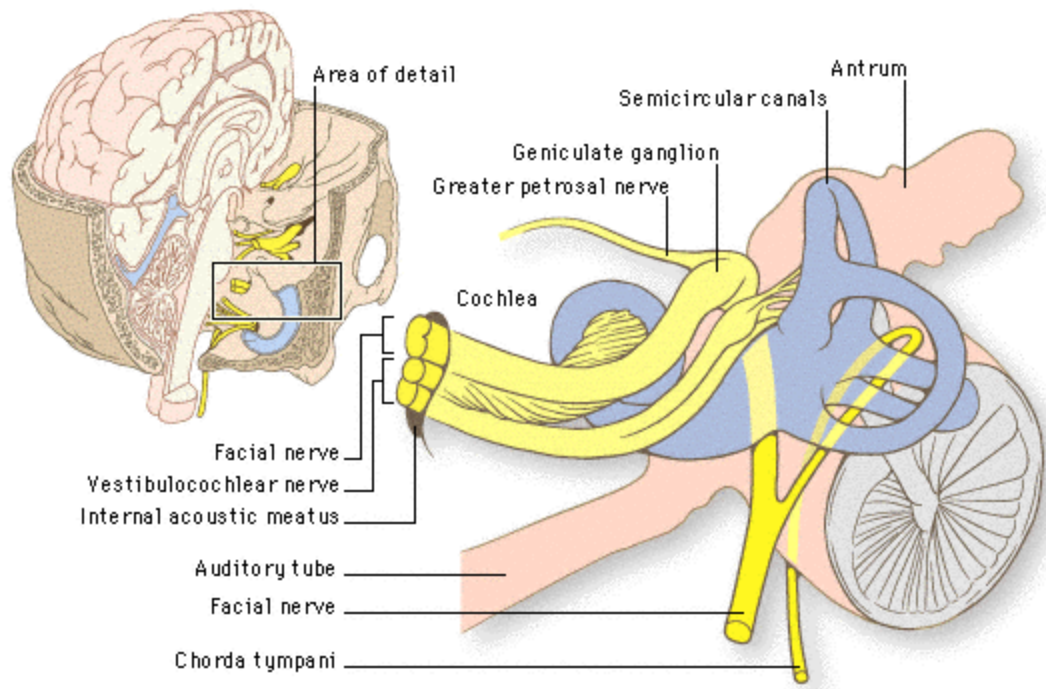


Figure (2. 6): Overview diagram of the facial nerve and vestibulocochlear nerve inside internal auditory canal. (Merchant, 2010).

2-5 The cerebellopontine angle cistern:

The cerebellopontine angle cistern is one of the large, interconnecting cerebrospinal fluid spaces (cisterns) at the base of the brain. It is a subarachnoid space whose medial margin is the pons, and whose lateral margins include the posterior petrous bone. Traversing the cistern are the facial (VIIth cranial) and the vestibulocochlear (VIIIth cranial) nerves. The anterior–inferior cerebellar artery, (AICA), a loop from which can occasionally enter the IAM, the petrosal vein of Dandy and the trigeminal (Vth cranial) nerve may also occur within the cistern.

2-6 pathology of Internal Auditory Canal and Cerebellopontine Angle:

2-6-1 Acoustic Neuroma:

Acoustic neuroma or vestibular schwannoma is the most common mass of the cerebellopontine angle. They are benign masses. These lesions may also remain stable for multiple years with no signs of growth on long-term follow-up. CT scans of acoustic schwannomas tend to show the features of a porus-centered mass, acute angles, IAC involvement. They also demonstrate the homogeneous nature of the mass. Calcifications

and central necrosis are rare, however, central clearing has been noted in some larger lesions. The density of AN on CT is similar to that of nearby brainstem, and more dense than surrounding CSF. If given IV contrast, the tumor will most likely show homogeneous uptake and turn very bright. A non-homogeneous uptake may be seen with previously treated lesions and large tumors. MRI is the study of choice if the diagnosis of AN is in question. On standard T1 images, the tumor should be relatively isointense to pons but more intense than CSF. On T2 images, the lesion should be mildly brighter than pons, but darker than CSF. After Gadolinium, the T1 sequence should show a very intense lesion, brighter than all other surrounding structures. (Alan, 2004)

2.6-2 Meningioma:

Meningioma is the second most common diagnosis of a primary CPA lesion. The meningioma is a vascular tumor, not homogeneous masses, and may show central clearing. Calcifications can be present in up to 25% and the significant finding is a “dural tail”. On CT scan, meningiomas may appear isodense to surrounding structures and it may also show calcifications within the tumor, which are highly suggestive of the diagnosis. MRI is the study of choice. T1 images will show a lesion near the intensity of pons, however, it may not be homogeneous, and may have a central hypointensity in larger lesions. On T2 images the lesion is between pons and CSF in intensity. After administration of gadolinium, the T1 image should show an intense lesion. (Alan, 2004)

2-6-3 cavernous hemangioma :

Cavernous hemangioma of the internal auditory canal is an extremely rare type of tumor.

2-6-4 Neurofibromatosis type 2 (NF2):

Is a tumor predisposition syndrome caused by germline or early embryonic heterozygous mutation of the *NF2* gene on chromosome 22q. The incidence is approximately one in 25,000 live births, and the disease demonstrates nearly 100% penetrance by the age of 60 years.¹ Manifestations of NF2 include central nervous system tumors (schwannomas, meningiomas, ependymomas, and rarely astrocytomas), ophthalmological lesions (cataracts, epiretinal membranes, and retinal hamartomas), and cutaneous lesions (skin tumors).¹ NF2 patients experience devastating consequences

and a decreased life expectancy as a result of tumor growth when the disease exhibits a severe phenotype, classically termed “Wishart” type NF2, that presents at an early age, with rapid tumor progression, and accompanied by various additional schwannomas, meningiomas, and ependymomas. This is in contrast to the milder NF2 phenotype, classically termed the “Gardner” type, that presents later in life with only bilateral VS that grow more slowly, or occasionally not at all, as a manifestation of the NF2 disease.² The propensity for NF2-related vestibular nerve schwannomas (VS) for infiltrating the auditory nerve rather than impinging against the wall of the internal auditory canal (IAC) was described in 1972 and 1980.^{3,4} These findings explained why these tumors could reach considerable size before hearing was affected and why removal of even small tumors could sacrifice the hearing due to the varying location of the auditory nerves within the tumor. The tendency of these tumors to invade the cochlea and vestibule has also been described.^{5,6} The presence of tumor within the inner ear, which can be determined with magnetic resonance imaging (MRI), compounds the difficulty with treatment of these tumors.⁷ NF2-related tumors may also invade the marrow spaces and pneumatic cells and cause destruction of the IAC bone.⁸ This invasive tendency is characteristic of the severe phenotype of NF2.

2-7 IAM Imaging and Pervious studies:

2-7-1 MRI:

Magnetic resonance (MR) is a measurement technique used to examine atoms and molecules. It is based upon the interaction between an applied magnetic field and a particle that possesses spin and charge. While electrons and other subatomic particles possess spin (or more precisely, spin angular momentum) and can be examined using MR techniques, formally known as Nuclear Magnetic Resonance, or NMR. Nuclear spin, or more precisely nuclear spin angular momentum, is one of several intrinsic properties of an atom and its value depends on the precise atomic composition. Every element in the Periodic Table except argon and cerium has at least one naturally occurring isotope that possesses nuclear spin. Thus, in principle, nearly every element can be examined using MR, and the basic ideas of resonance absorption and relaxation

are common for all of these elements. The precise details will vary from nucleus to nucleus and from system to system (brain, 2015).

Magnetic resonance imaging (MRI) of the internal acoustic canal is the standard diagnostic tool for a wide range of indications in patients. With the technological advances in magnetic resonance (MR) imaging, the course of the facial nerve and vestibulocochlear nerves from the brain stem to the internal acoustic canal (IAC) became more visible to the radiologists. These nerves have important roles in hearing, balance, taste sensation, and parasympathetic function. The area crossed by the facial nerve and vestibulocochlear can be involved in various pathologies, such as neurogenic tumors, glomus tumors, leptomeningeal disease (inflammatory and metastatic diseases), meningiomas, and neurovascular compression. (Agirdir, 2001) (Brunsteins, 1995).

Routine MR imaging sequences provide optimal softtissue resolution, but spatial resolution necessary to define cranial nerves (CNs) may be insufficient with this technique. 3D fast imaging employing steady-state acquisition (FIESTA) sequences provides much higher spatial resolution and clearer depiction of small structures such as CNs especially within the cisternal spaces. The 3DFIESTA is an ultrafast pulse sequence that produces highresolution images with outstanding image contrast between the cerebrospinal fluid, vessels and CNs and high signal-tonoise-ratio, making thereby small structures conspicuous. (Driscoll,2001).

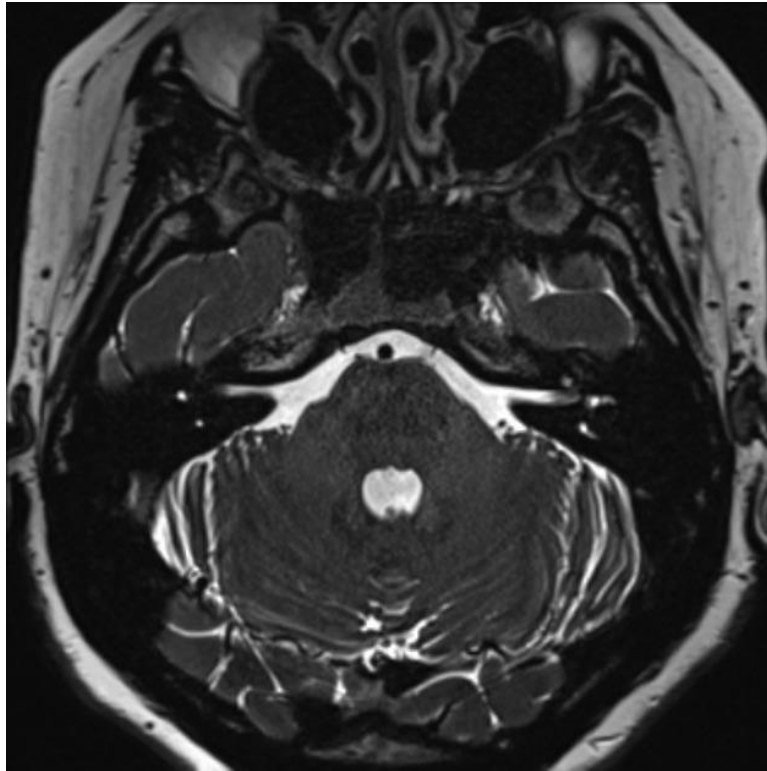


Figure (2. 7): Overview diagram of MRI image axial t2 section at level of IAM showing bundle of nerve.

2-7-2 CT:

Micro-computed tomography (micro-CT) high resolution images of the fundus of internal acoustic meatus (FIAM) and characterize the normal appearance of its singular areas which are places of passage of numerous anatomical structures. By using micro-CT we obtain detailed volume rendering images presenting topography of the FIAM in 3-dimensional (3D) space. 3D reconstructions obtained from micro-CT scans can precisely demonstrate all areas of the FIAM (facial nerve area, cochlear area, superior and inferior vestibular areas, singular foramen). Application of this technique allows finding out new anatomical structures like the foramen of the transverse crest, which is not described in literature. (Folia Morphol 2015; 74, 3: 352–358)

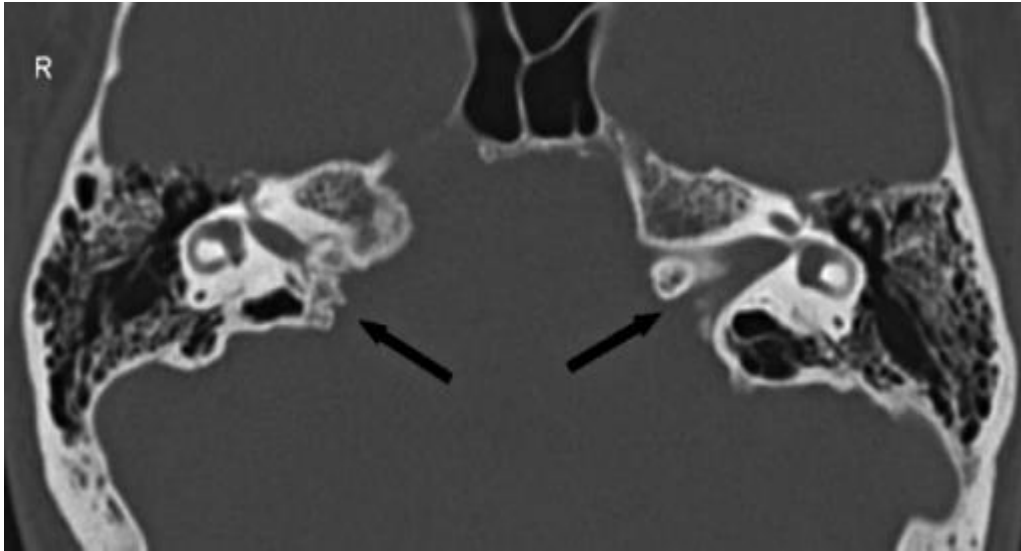


Figure (2. 8): Overview diagram of CT image axial section at level of IAM.

2-7-3 Previous studies:

Sergio Ricardo Marques et al in 2012 studied role of CT in characterize the morphology variation of the internal auditory canal (IAC). this prospective study done at Department of Morphology and Genetics, Sao Paulo Federal University, Sao Paulo, Brazil, Department of Diagnosis by Image, Sao Paulo Federal University, Sao Paulo, Brazil , Institutes of Physics, Sao Paulo Federal University, Sao Paulo, Brazil.

CT images of the IAC of 110 normal subjects aged 1 to 92 years (mean age, 46.5 years) of both genders.

The shapes observed in children and adults were funnel-shaped (74% and 58.3%, respectively), cylindrical (22% and 30.9%, respectively) and bud-shaped (4% and 10.8%, respectively). The measurements by CT in children were: area= 50.30 mm², OW = 7.53 mm, length = 11.17 mm, VD = 4.82 mm and the distance between the IAC and the vestibular aqueduct (VA) = 12.63 mm. In adults, the measurements were: area = 44.64 mm², OW = 7.10 mm, length = 9.84 mm, VD = 4.47 mm and the distance between IAC and VA = 11.17 mm.

Nezahat Erdogan et al in 2013 studied role of MRI assessment of internal acoustic canal variations using 3D-FIESTA sequences. The study group comprised 187 patients (104 women, 83 men; mean age, 48.8 years) in whom temporal bone MR imaging was

performed for tinnitus, vertigo, unilateral hearing loss or facial neuritis. These patients were consecutively referred to our department for temporal bone MR imaging and evaluated between November 2009 and July 2010. A total of 374 temporal bones from 187 patients were evaluated by MRI in our study. Facial and vestibulocochlear nerves and vascular structures were visualized with 3D FIESTA sequences.

M. Kozerska, J. Skrzat in 2014 studied Anatomy of the fundus of the internal acoustic meatus — micro-computed tomography study at Department of Anatomy, Jagiellonian University, Collegium Medicum, Krakow, Poland.

Morphological study of anatomy of the FIAM was performed on 10 dry temporal bones: 5 samples derived from adult individuals of female sex, 2 samples were of male sex and 3 samples derived from infant skulls of unknown sex. All the examined bones were well preserved, presented normal anatomy and were not deformed. The fundus of IAM was identified as lateral end of the IAM communicating the posterior cranial fossa with the labyrinth. The internal acoustic aperture being the inlet to IAM was easily recognized on the posterior surface of the pyramid of the temporal bone and reconstructed from micro-CT scans in all examined samples. These topographical relationships were visualized by volume rendering and overall morphology of the petrous bone with visible inlet to the IAM was presented.

2-8 Computer Tomography Instrumentation and Technique:

Computed tomography (CT) is a technology that uses computer-processed x-rays to produce tomographic images of specific areas of the scanned object, allowing the user to see what is inside it without cutting it open. Digital geometry processing is used to generate a three-dimensional image of the inside of an object from a large series of two-dimensional radiographic images taken around a single axis of rotation. Medical imaging is the most common application of x-ray CT. Its cross sectional images are used for diagnostic and therapeutic purposes in various medical disciplines. (Adrian, 2011).

2-8-1 Modern Computed Tomography Modalities

In all original CT scanners (1974 to 1987), the x-ray power was transferred to the x-ray tube using high voltage cables wrapped around an elaborate set of rotating drums and pulleys. (J.A Miller et al, 2000)

The rotating frame (or gantry) would spin 360° in one direction and make an image (or a slice), and then spin 360° back in the other direction to make a second slice. In between each slice, the gantry would come to a complete stop and then reverse directions while the patient table would be moved forward by an increment equal to the slice thickness.

(J.A Miller et al, 2000) In the mid 1980's, an innovation called the power slip ring was developed so that the elaborate x-ray cable and drum system could be abandoned. The slip ring allows electric power to be transferred from a stationary power source onto the continuously rotating gantry. State of the art CT scanners with slip rings can now rotate continuously and do not have to slow down to start and stop. The innovation of the power slip ring has created a renaissance in CT called spiral or helical scanning. (Euclid, 2000)

These spiral CT scanners can now image entire anatomic regions like the lungs in a quick 20 to 30 second breath hold. Instead of acquiring a stack of individual slices which may be misaligned due to slight patient motion or breathing (and lung/abdomen motion) in between each slice acquisition, spiral CT acquires a volume of data with the patient anatomy all in one position. This volume data set can then be computer-reconstructed to provide three dimensional pictures of complex blood vessels like the renal arteries or aorta. 3D CT images from volume data allow surgeons to visualize complex fractures, for example of facial trauma, in three dimensions and can help them plan reconstructive surgery. (Euclid, 2000) Additional major advance in CT imaging came in the early 1990s with the introduction of helical/spiral CT imaging and its slip-ring technology. In order to avoid anatomical gaps in the data set, the helical pitch is set lower, that used for general body imaging. Thus the dose to the patient is higher. Nevertheless, the ability to reconstruct images in multiple phases from the same high-resolution data set can provide important information. Sub millimeter slices, as

small as 0.5 mm, can be used to achieve a high spatial resolution. (Kalendar et al, 1990).

Figure 2-9

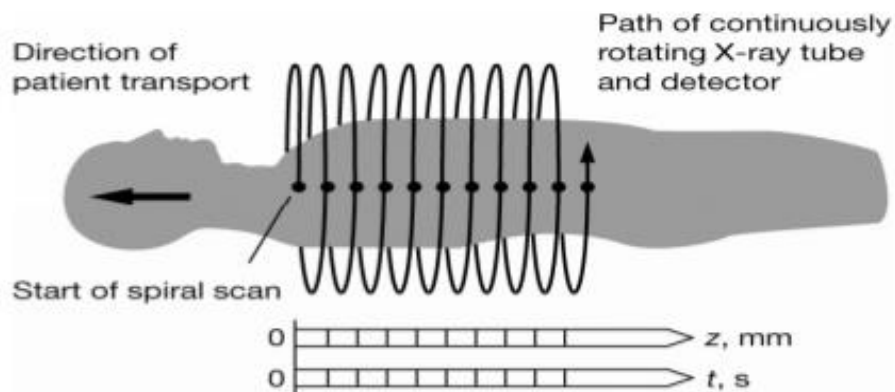


Figure (2-9) shows: show spiral CT principle. (Euclid,2000)

2-8-2 Positioning considerations for IAM imaging:

CT scanning of the head is typically used to detect infarction, tumors, calcifications, hemorrhage and bone trauma. Of the above, hypodense (dark) structures indicate infarction or tumors, hyperdense (bright) structures indicate calcifications and hemorrhage and bone trauma can be seen as disjunction in bone windows. Ambulances equipped with small bore multi-sliced CT scanners respond to cases involving stroke or head trauma. (Herman.2009) CT Head patient supine AP and lateral scouts, no gantry angle, Helical mode should be used routinely for adult head CT scans. Only use axial mode when you cannot move the patient's head into proper position (trauma, cervical collar, rigid neck). Tilt the patients head so that a line connecting the lateral canthus of the eye and the EAC is perpendicular to the CT tabletop. Use axial mode and angle the gantry if you cannot place the patient's head within 15 degrees of the proper setup angle, start scans at the bottom of C1 and scan through the top of the head (Gentry.Ranallo, 2009)

Coronal sections Temporal Bone without contrast done; Patient Supine, AP and lateral scouts taken, no gantry angle, only use 64 slice scanners. Patient Positioning: Tilt the patient's head so that a line connecting the lateral canthus of the eye and the EAC is perpendicular to the CT table top , Start scans at the mastoid tip and finish at the top of

the petrous bone and Recon 1 and Retro Recons: Preferred 20 cm (Range 18-22 cm), Recon 2 and 3 of TB: 9.6 cm, choose the CT scan factors on the scanner for the proper age range of the patient (Gentry.Ranallo, 2009) (figure 2-10)

For child: (3 – 6 years) Recon 1: 2.5 mm axial images using a bone algorithm And infant: (0 – 3 years) Recon 2 & 3: Obtain left and right 0.625 mm temporal bone axial images with a DFOV of 9.6 cm. Perform 1 additional Retro Recons to get the following axial images of the entire scan range: At 20 cm DFOV, standard algorithm, .5 mm slice thickness, 1.25 mm increment, (WW/WL:400/30) and 1 mm by 1 mm 2D-reformats done in the coronal, Stenver's, and Pöschl planes of each temporal one using Recon 2 & 3 as source images. (Gentry.Ranallo, 2009)

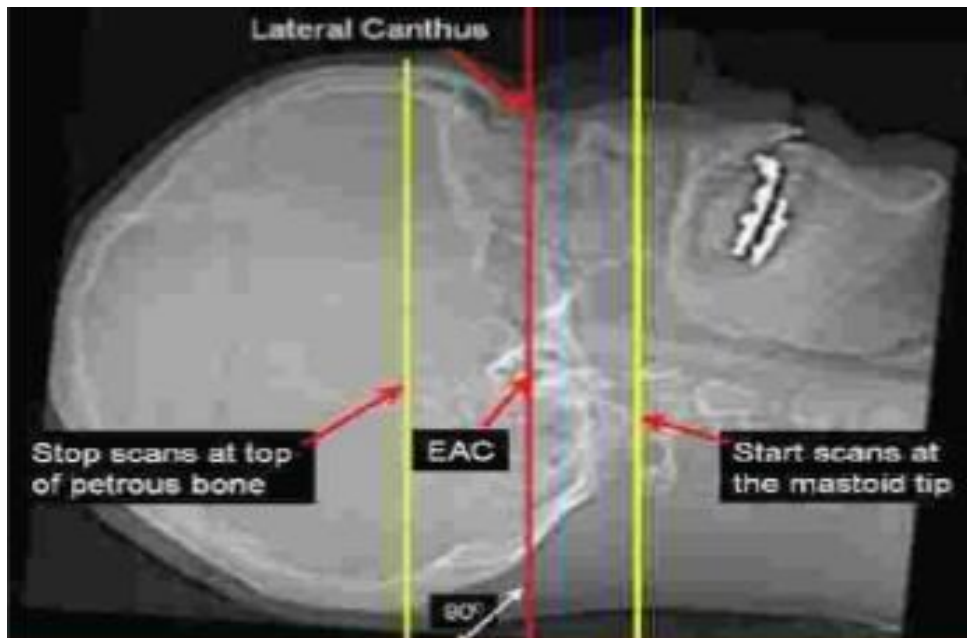


Figure 2.10 lateral scout determination of start and end scan level (Gentry-Ranallo,2009)

Chapter three

Materials and Methods

3-1 Materials:

3-1-1 Subject:

A total of 80 subjects were retrospectively investigated for Sudanese patients were included, 160 Rt and Lt ears, in both gender, Their age ranged from 1 to 90 years. There were adult children. Males and females .they divided to two group: group a children 1-15 group B adults 15-90. CT scan study of the temporal bone was performed for all the patients for following indication: headache, tinnitus, hearing loss, mild acute recurrent otitis and other symptoms of unknown non-congenital and non-anatomical etiology.

3-1-2 Area and duration:

The data will be collected in Khartoum state hospital from Modern Medical Center (MMC) from December 2018 to June 2019.

3-1-3 Equipment:

American GE lightspeed 64 slice CT scanner and structures using a system of digital image processing.

3-1-4 including Criteria

- 1- Sudanese
- 2- In the age of (1 – 90) years
- 3- Normal hearing grade

3-1-5 Exclusion criteria

Subjects with tumor lesion, inflammatory process, congenital anatomical anomalies and surgical manipulation or implantation.

3-2 Methods:

3-2-1 Technique protocol:

The tomography (GE 64 slice CT scanner) was used for obtaining the images. The protocol included taking shots from the axial plane with the patients lying on their back. The cuts were 1.0 mm thickness and taken at 1.0 mm intervals. The images were acquired by parameters of 120 Kvp, 180mAs, exposure time of 1.00s and a matrix of 512×512 .

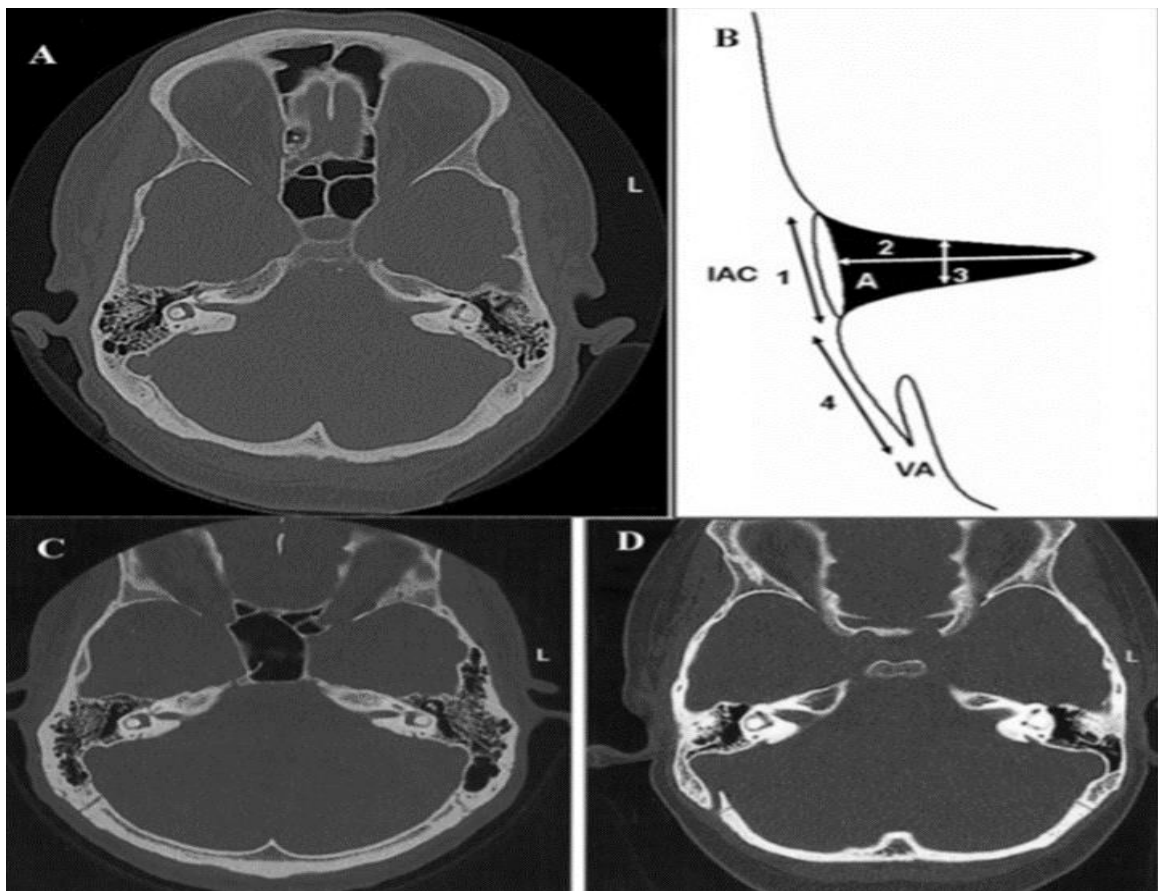


Figure (3-1) A,C,D CT imaging axial cut at level of IAM , D present diameters of the canal .

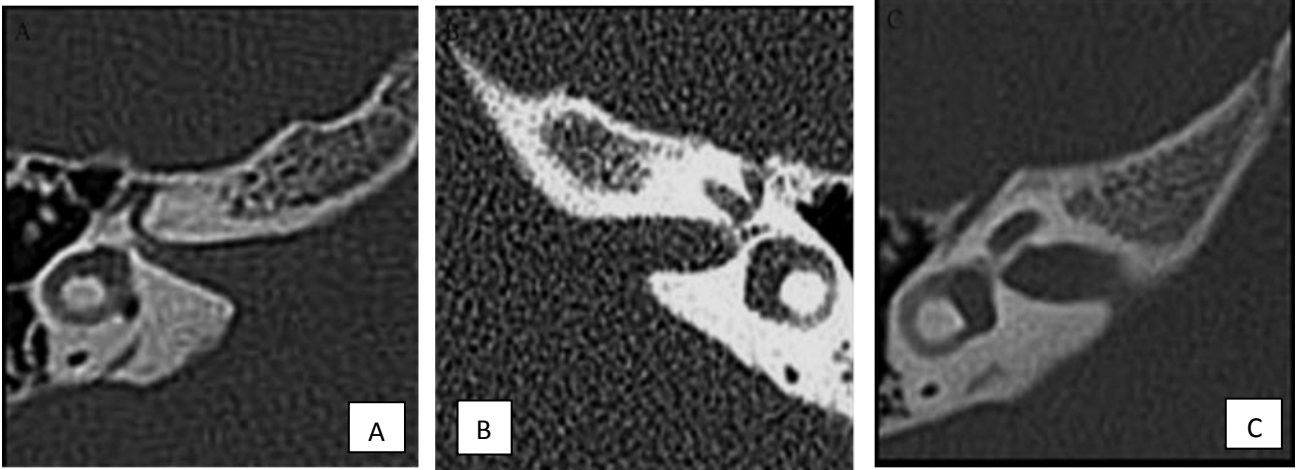


Figure 3-2 types of shapes observed for the IAC in CT images, A funnel shape, B cylinder shape, C bud shape.

3-2-2 Data collection

The following features were measured: opening width, longitudinal length from the opening to the end of the canal along its axis, AP diameter of the length of the canal, distance between the openings of the IAC and vestibular aqueduct, and selected area of the IAC figure 3-1, gender and age .The shapes of the IAC were defined as cylindrical, funnel shaped or bud-shaped. Figure 3-2

3.2.3 Data analysis:

Descriptive statistics will used to describe the study variables, using the Statistical Package Software (SPSS) to analyze variables.

Chapter four

Results

Table (4.1) frequency distribution of gender

Gender	Frequency	Percent	Valid Percent	Cumulative Percent
Female	41	51.2	51.2	51.2
Male	39	48.8	48.8	100.0
Total	80	100.0	100.0	

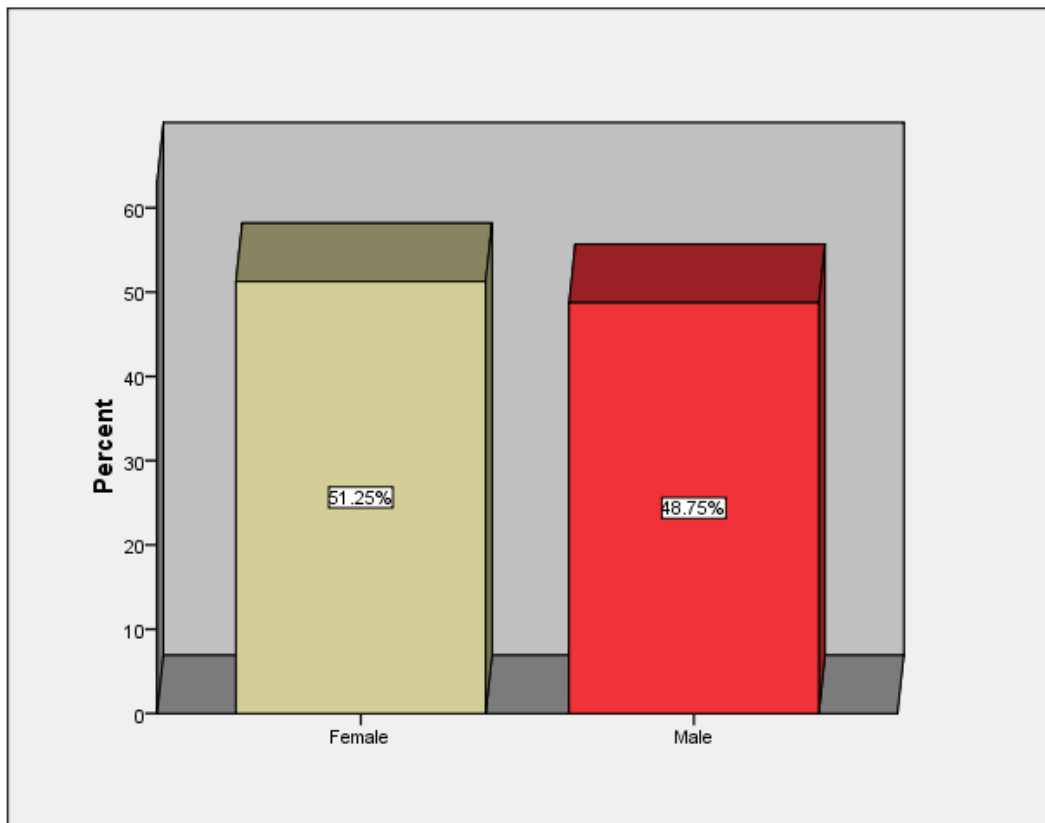


Figure (4.1) frequency distribution of gender

Table (4.2) frequency distribution of age \years

Age \years	Frequency	Percent	Valid Percent	Cumulative Percent
3-17	25	31.2	31.2	31.2
18-37	22	27.5	27.5	58.8
38-47	4	5.0	5.0	63.8
48-57	9	11.2	11.2	75.0
58-67	4	5.0	5.0	80.0
68-77	7	8.8	8.8	88.8
78-90	9	11.2	11.2	100.0
Total	80	100.0	100.0	

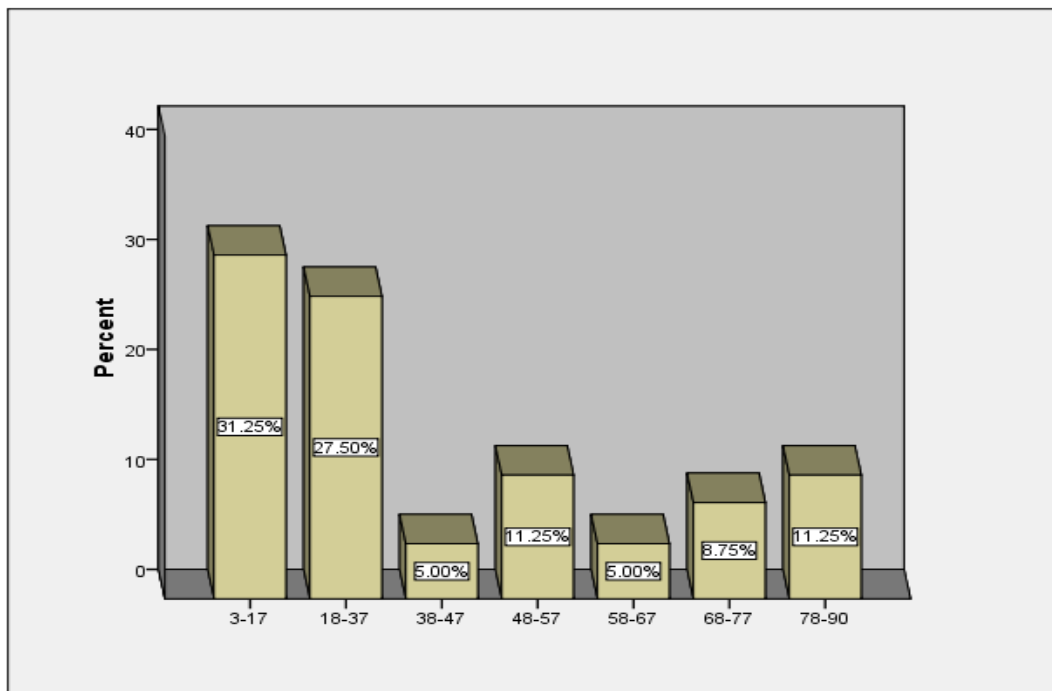


Figure (4.2) frequency distribution of age \years

Table (4.3) descriptive statistic of age \years and measurements (min, max, mean± Std. Deviation)

Variables	N	Minimum	Maximum	Mean	Std. Deviation
Age	80	3	90	37.55	26.509
Ow right	80	3	9	6.01	1.278
Ow left	80	4	9	6.56	1.395
Length right	80	5	14	10.39	1.695
Left length	80	6	15	10.18	1.667
AP right	80	3	7	4.23	.954
AP left	80	2	8	4.52	1.102
Area right	80	20.3	70.5	42.297	9.4766
Area left	80	23.6	72.0	41.643	9.2190
Right IAC\VA	80	4	18	12.05	2.510
LT IAC\VA	80	7	19	13.05	2.823
Valid N (listwise)	80				

Table (4.4) frequency distribution of shape

Shape	Frequency	Percent	Valid Percent	Cumulative Percent
Bud	18	22.5	22.5	22.5
Cylindrical	26	32.5	32.5	55.0
Funnel	36	45.0	45.0	100.0
Total	80	100.0	100.0	

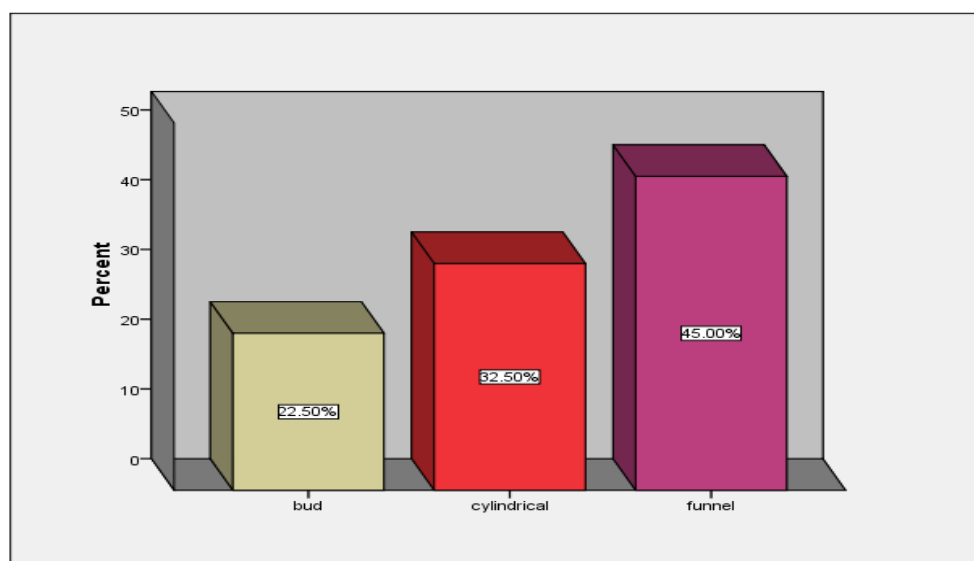


Figure (4.3) frequency distribution of shape

Table (4.5) correlation between age and measurements of right internal auditory canal

		Age	Ow rt	RT L	RT AP	RT area	RT IAC\VA
Age	Pearson Correlation	1	-.103-	-.196-	-.013-	-.098-	.295**
	Sig. (2-tailed)		.365	.081	.906	.385	.008
Ow rt	Pearson Correlation	-.103-	1	.255*	.288**	.115	.055
	Sig. (2-tailed)	.365		.023	.010	.311	.628
RT L	Pearson Correlation	-.196-	.255*	1	.133	.369**	-.025-
	Sig. (2-tailed)	.081	.023		.239	.001	.823
RTAP	Pearson Correlation	-.013-	.288**	.133	1	.248*	.053
	Sig. (2-tailed)	.906	.010	.239		.027	.638
RT area	Pearson Correlation	-.098-	.115	.369**	.248*	1	.196
	Sig. (2-tailed)	.385	.311	.001	.027		.081
RT IAC\VA	Pearson Correlation	.295**	.055	-.025-	.053	.196	1
	Sig. (2-tailed)	.008	.628	.823	.638	.081	
	N	80	80	80	80	80	80
**. Correlation is significant at the 0.01 level (2-tailed).							
*. Correlation is significant at the 0.05 level (2-tailed).							

Table (4.6) correlation between age and measurements of left internal auditory canal

		Age	Ow lt	L T L	LT AP	LT area	L IAC\VA
Age	Pearson Correlation	1	.026	-.121-	-.044-	-.282*	.297**
	Sig. (2-tailed)		.818	.286	.700	.011	.008
Ow lt	Pearson Correlation	.026	1	.295**	.522**	.234*	.192
	Sig. (2-tailed)	.818		.008	.000	.036	.088
LT L	Pearson Correlation	-.121-	.295**	1	.321**	.225*	.240*
	Sig. (2-tailed)	.286	.008		.004	.045	.032
LTAP	Pearson Correlation	-.044-	.522**	.321**	1	.381**	.231*
	Sig. (2-tailed)	.700	.000	.004		.000	.039
LT area	Pearson Correlation	-.282*	.234*	.225*	.381**	1	.164
	Sig. (2-tailed)	.011	.036	.045	.000		.146
LT IAC\VA	Pearson Correlation	.297**	.192	.240*	.231*	.164	1
	Sig. (2-tailed)	.008	.088	.032	.039	.146	
	N	80	80	80	80	80	80
*. Correlation is significant at the 0.05 level (2-tailed).							

Table (4.7) compares mean measurements of internal auditory canal in different gender

a. Mean

Group Statistics					
Measurements	Gender	N	Mean	Std. Deviation	Std. Error Mean
Ow rt	Male	39	5.82	1.275	.204
	Female	41	6.20	1.269	.198
Ow left	Male	39	6.85	1.443	.231
	Female	41	6.29	1.309	.204
RT L	Male	39	10.38	1.756	.281
	Female	41	10.39	1.656	.259
LT L	Male	39	10.18	1.537	.246
	Female	41	10.17	1.801	.281
RT AP	Male	39	4.49	.970	.155
	Female	41	3.98	.880	.137
LT AP	Male	39	4.79	1.105	.177
	Female	41	4.27	1.049	.164
RT area	Male	39	44.469	9.5202	1.5245
	Female	41	40.230	9.0711	1.4167
LT area	Male	39	43.659	10.0647	1.6116
	Female	41	39.726	7.9933	1.2483
RT IAC\VA	Male	39	11.97	2.786	.446
	Female	41	12.12	2.249	.351
LT IAC\VA	Male	39	13.03	2.833	.454
	Female	41	13.07	2.849	.445

a. t. test for compare mean measurements of internal auditory canal in different gender

	t-test for Equality of Means						
	t	df	Sig. (2-tailed)	Mean Difference	Std. Error Difference	95% Confidence Interval of the Difference	
						Lower	Upper
Ow rt	-1.317-	78	.192	-.375-	.284	-.941-	.192
	-1.317-	77.765	.192	-.375-	.285	-.941-	.192
Ow left	1.799	78	.076	.553	.308	-.059-	1.166
	1.795	76.337	.077	.553	.308	-.061-	1.168
RT L	-.015-	78	.988	-.006-	.382	-.765-	.754
	-.015-	77.083	.988	-.006-	.382	-.767-	.755
LT L	.023	78	.981	.009	.375	-.738-	.756
	.023	77.109	.981	.009	.374	-.736-	.753
RT AP	2.473	78	.016	.512	.207	.100	.923
	2.467	76.343	.016	.512	.207	.099	.925
LT AP	2.187	78	.032	.527	.241	.047	1.006
	2.184	77.201	.032	.527	.241	.046	1.007
RT area	2.039	78	.045	4.2387	2.0785	.1007	8.3768
	2.037	77.245	.045	4.2387	2.0811	.0950	8.3825
LT area	1.940	78	.056	3.9326	2.0269	-.1026-	7.9679
	1.929	72.488	.058	3.9326	2.0386	-.1307-	7.9960
RT IAC\VA	-.261-	78	.795	-.148-	.565	-1.272-	.977
	-.260-	73.051	.796	-.148-	.568	-1.279-	.984
LT IAC\VA	-.075-	78	.941	-.048-	.636	-1.313-	1.218
	-.075-	77.843	.941	-.048-	.635	-1.313-	1.218

Table (4.8) compare mean measurements of internal auditory canal in different age group

Age \years		Ow lt	Ow rt	Lt L	Rt L	Lt AP	Rt AP	Lt area	Rt area	Lt iac\va	Rt iac\va
3-17	Mean	6.32	5.76	10.04	10.32	4.60	4.20	42.677	42.300	11.96	10.48
	Std. D	1.215	.970	1.989	1.796	1.22	.913	9.8000	9.2785	2.389	2.29
18-37	Mean	6.91	6.73	10.95	11.14	4.59	4.36	45.426	44.784	13.36	13.0
	Std. D	1.601	1.420	1.430	1.457	1.22	1.13	11.234	11.496	2.718	2.07
38-47	Mean	6.50	5.50	10.00	10.50	4.75	4.25	41.872	41.292	12.25	11.0
	Std. D	1.915	.577	.816	1.291	.957	.957	5.0009	9.1479	2.986	3.55
48-57	Mean	6.56	6.00	10.00	10.11	4.44	4.22	39.402	40.157	13.22	12.4
	Std. D	1.333	1.225	1.225	1.167	.726	.833	7.9014	10.162	2.539	1.94
58-67	Mean	6.00	5.25	9.00	9.75	4.00	3.75	36.390	34.850	14.25	13.2
	Std. D	2.000	2.062	2.160	2.062	.816	.500	3.5259	4.8898	4.349	3.77
68-77	Mean	6.57	6.00	9.29	10.29	4.29	4.14	36.864	43.091	12.57	12.4
	Std. D	1.397	1.528	1.254	1.380	1.25	.900	5.4808	8.3264	3.259	2.63
78-90	Mean	6.67	5.56	10.11	9.33	4.56	4.22	37.719	41.484	15.33	13.3
	Std. D	1.118	.882	1.537	2.236	1.01	1.09	4.6206	5.8562	2.500	1.58
Total	Mean	6.56	6.01	10.18	10.39	4.52	4.23	41.643	42.297	13.05	12.05
	N	80	80	80	80	80	80	80	80	80	80
	Std. D	1.395	1.278	1.667	1.695	1.10	.954	9.2190	9.4766	2.823	2.51
P value		0.842	0.079	0.163	0.191	0.954	0.96	0.149	0.609	0.076	0.005

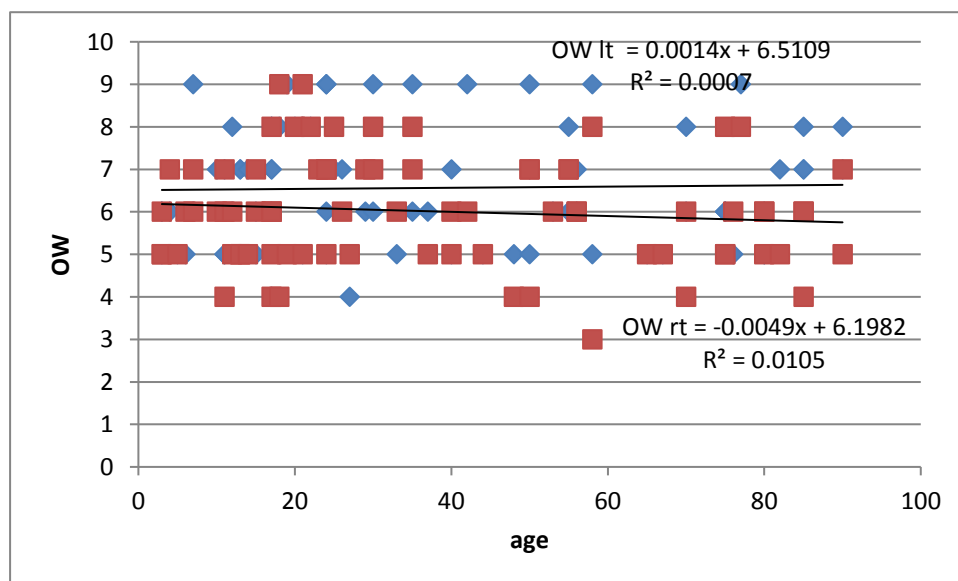


Figure (4.4) scatterplot shows relationship between age and opening width

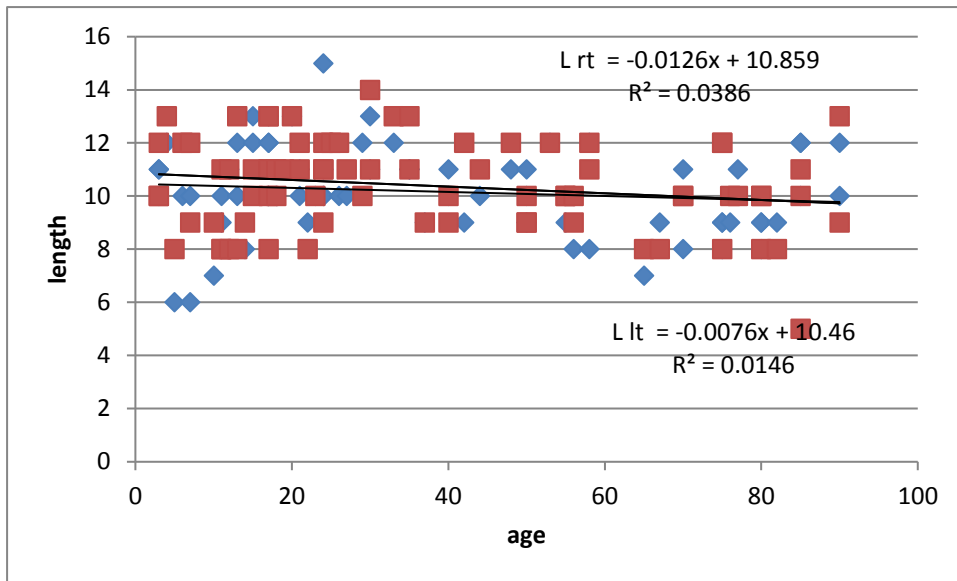


Figure (4.5) scatterplot shows relationship between age and length

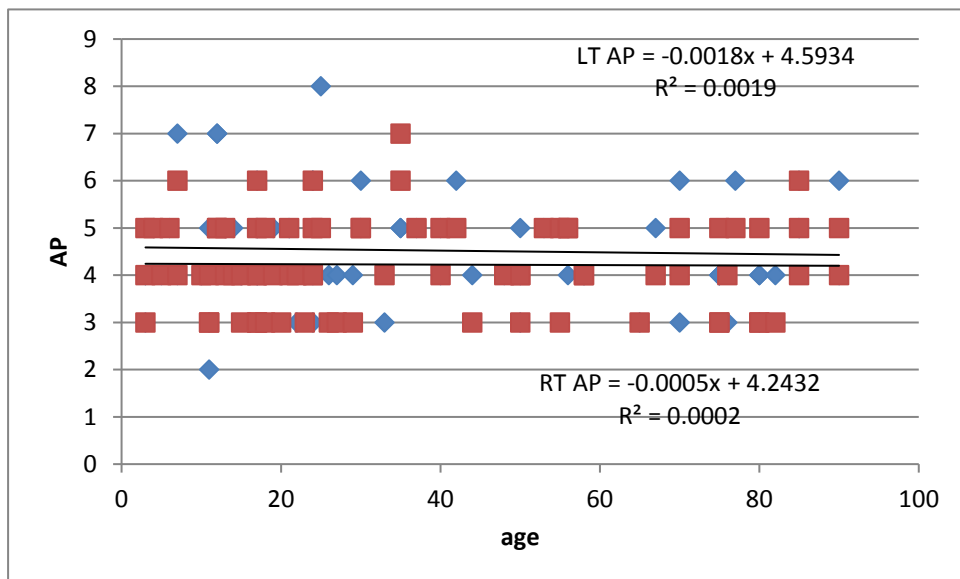


Figure (4.6) scatterplot shows relationship between age and AP

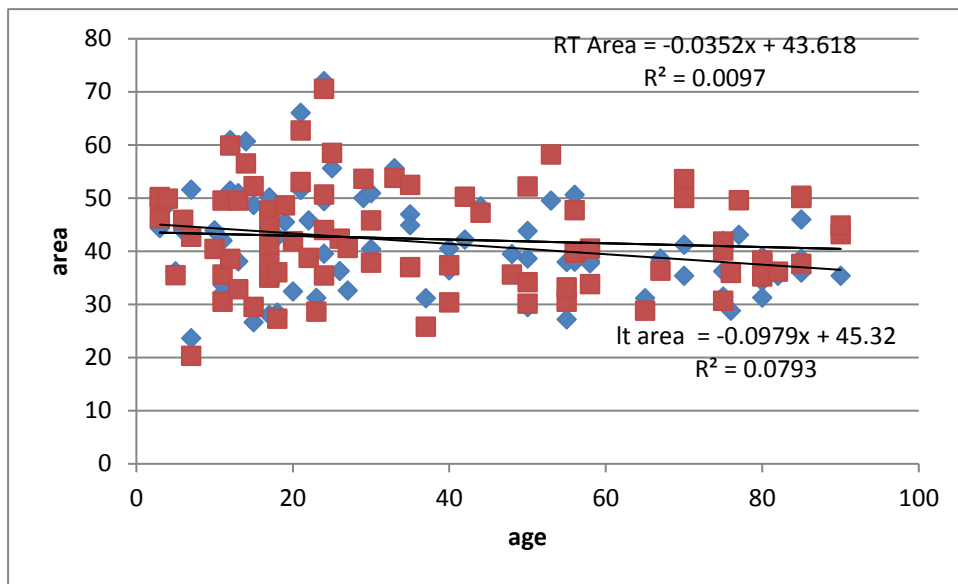


Figure (4.7) scatterplot shows relationship between age and area

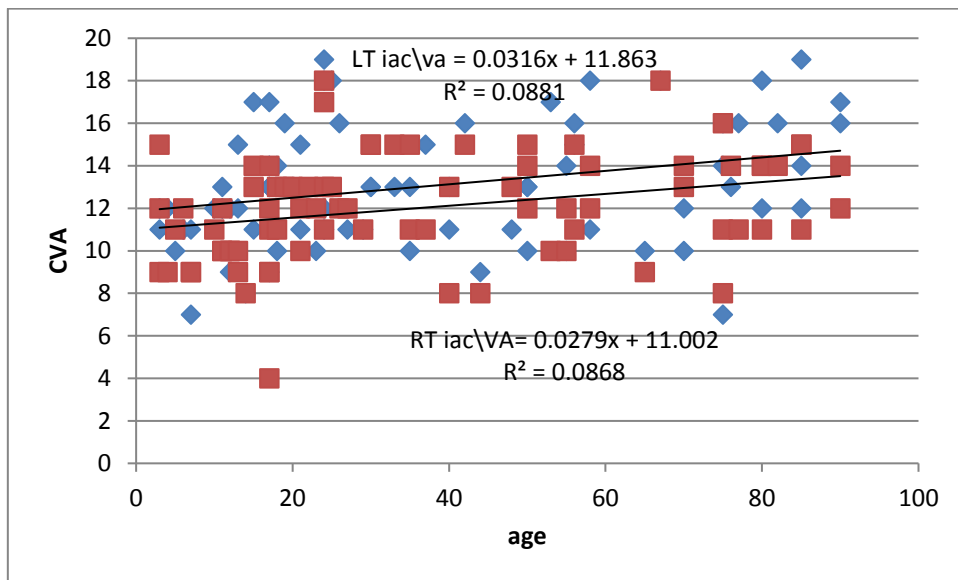


Figure (4.8) scatterplot shows relationship between age and IAC\VA

Table (4.9) compares mean measurements of internal auditory canal in different in the children and adult

a. Mean

Group Statistics

	Cccc	N	Mean	Std. Deviation	Std. Error Mean
Owl	Children	25	6.32	1.215	.243
	Adult	55	6.67	1.466	.198
Owrt	Children	25	5.76	.970	.194
	Adult	55	6.13	1.389	.187
Ll	Children	25	10.04	1.989	.398
	Adult	55	10.24	1.515	.204
Rl	Children	25	10.32	1.796	.359
	Adult	55	10.42	1.663	.224
Lap	Children	25	4.60	1.225	.245
	Adult	55	4.49	1.052	.142
Rtap	Children	25	4.20	.913	.183
	Adult	55	4.24	.981	.132
Ltarea	Children	25	42.677	9.8000	1.9600
	Adult	55	41.174	8.9963	1.2131
Rtare	Children	25	42.300	9.2785	1.8557
	Adult	55	42.295	9.6499	1.3012
ltiac\va	Children	25	11.96	2.389	.478
	Adult	55	13.55	2.886	.389
rtiac\va	Children	25	10.48	2.293	.459
	Adult	55	12.76	2.285	.308

b. test for compare mean measurements of internal auditory canal in children and adult

	t-test for Equality of Means						
	T	df	Sig. (2-tailed)	Mean Difference	Std. Error Difference	95% Confidence Interval of the Difference	
						Lower	Upper
Owl	-1.049-	78	.297	-.353-	.336	-1.022-	.317
	-1.126-	55.481	.265	-.353-	.313	-.980-	.275
Owrt	-1.195-	78	.236	-.367-	.307	-.979-	.245
	-1.363-	64.639	.178	-.367-	.270	-.906-	.171
LI	-.486-	78	.628	-.196-	.404	-1.001-	.608
	-.439-	37.175	.663	-.196-	.447	-1.102-	.710
RI	-.239-	78	.812	-.098-	.411	-.917-	.721
	-.232-	43.420	.818	-.098-	.424	-.952-	.756
Lap	.408	78	.684	.109	.267	-.423-	.641
	.385	40.755	.702	.109	.283	-.463-	.681
Rtap	-.157-	78	.876	-.036-	.232	-.498-	.425
	-.161-	49.702	.873	-.036-	.225	-.489-	.416
Itarea	.674	78	.503	1.5030	2.2314	-2.9395-	5.9454
	.652	43.097	.518	1.5030	2.3050	-3.1452-	6.1512
Rtare	.002	78	.998	.0049	2.3004	-4.5749-	4.5847
	.002	48.221	.998	.0049	2.2664	-4.5515-	4.5613
Itiac\ va	-2.397-	78	.019	-1.585-	.661	-2.902-	-.269-
	-2.573-	55.535	.013	-1.585-	.616	-2.820-	-.351-
rtiac\ va	-4.139-	78	.000	-2.284-	.552	-3.382-	-1.185-
	-4.133-	46.348	.000	-2.284-	.553	-3.396-	-1.172-

Table (4.10) correlation between right and left sides of internal auditory canal

		owl	ll	lap	ltarea	ltiac\va
Owrt	Pearson Correlation	.422**	.350**	.283*	.087	-.025-
	Sig. (2-tailed)	.000	.001	.011	.444	.828
	N	80	80	80	80	80
Rl	Pearson Correlation	.233*	.518**	.269*	.310**	.033
	Sig. (2-tailed)	.037	.000	.016	.005	.772
	N	80	80	80	80	80
Rtap	Pearson Correlation	.360**	.253*	.608**	.237*	.155
	Sig. (2-tailed)	.001	.023	.000	.035	.168
	N	80	80	80	80	80
Rtare	Pearson Correlation	.246*	.363**	.404**	.826**	.195
	Sig. (2-tailed)	.028	.001	.000	.000	.084
	N	80	80	80	80	80
rtiac\va	Pearson Correlation	.136	.122	.032	.148	.548**
	Sig. (2-tailed)	.227	.281	.781	.190	.000
	N	80	80	80	80	80
**. Correlation is significant at the 0.01 level (2-tailed).						
*. Correlation is significant at the 0.05 level (2-tailed).						

Chapter five

Discussion, conclusion and recommendations

5.1 Discussion

The study was interesting to evaluate the internal auditory canals dimension and shape of normal Sudanese people in different age use computed tomography.

The study had done over both gender male and female with percentage (48.8%, 51.2%) respectively. table (4.1). with mean age of 37.55 ± 26.5 year .table (4.3).thier age were classified with an interval 9 of year as descriptive graph showed in figure (4.1).

The variables were the mean right and left internal auditory canal : opening width measured ($6.01 \text{ mm} \pm 1.2\text{mm}$, $6.56 \text{ mm} \pm 1.3\text{mm}$) , the length measured ($10.3\text{mm} \pm 1.6\text{mm}$, $10.18\text{mm} \pm 1.6\text{mm}$) , AP diameters were ($4.23\text{mm} \pm 0.9\text{mm}$, $4.5\text{mm} \pm 1.1\text{mm}$), the area measured ($42.2\text{mm} \pm 9.4\text{mm}$, $41.6 \pm 9.2\text{mm}$) and the distance between the opining of IAC and the vestibular aqueduct were ($12.05\text{mm} \pm 2.5\text{mm}$, $13.05\text{mm} \pm 2.8\text{mm}$)respectively . table (4.3) .with no significant differences were noted in both sides. These were the standard measures of Sudanese normal IAC found by this study.

The IAC presented different shapes,in this study, the funnel -shape IAC was the most common on 45% followed by the cylindrical -shape 32.5 % and the bud-shape 22.5%. table (4.4) , figure (4.3).

Also this study had explained:

There is no significant between age and measurement of right IAM ,more than 0.05 except for age and IAC/VA less than 0.01 significant level . and there is a weak negative correlation between them except for age and IAC/VA there is a weak positive correlation . table (4.5).

There is no significant between age measurement of left IAM at 0.05 significant level except for age and area and age and IAC/VA less than 0.05 at 0.05 significant level . and there is a weak negative correlation between them except for age and IAC/VA there is a weak positive correlation . table (4.6).

In general measurement of the mean variables of internal auditory canal according to the gender were more in male than females . table (4.7) a.

There is no significant difference in measurements in different gender p more than 0.05 except for AP diameter right and AP diameter left measurement p less than 0.05. table (4.7)b.

Table (4.8) clarified there is no significant different between the age group in the measurement p more than 0.05.

In the general the measurement of the variable of IAC between children and adult the mean of the variables is more in adult than children table (4.9) a.

And there is no significant difference between opening width , length of canal ,AP diameter and areas between children and adult of both genders .however , there are statistical differences between its distance of IAC /VA in adult and children .table (4.9)b

Table (4.10) represented there is no different between the left and the right side of internal auditory canal.

A Sergio Ricardo study of 2012 analyzed 110 human temporal bones of individuals aged 1to 92 years and found there is variations in the shapes of the human IAC ,the most frequent shape was the funnel-shaped (58.3%), followed by the cylindrical (30.9%) and finally the bud-shaped (10.8%).which is same found in this study .

According to the standardized criteria for polytomography classification in 300 normal subjects where 180 were male and 120 were female (mean age, 47 years; range, 14-77 years), the shape of the internal acoustic meatus was cylindrical in 436 ears (72.7%), bud-shaped in 137 ears (22.8%) and funnel-shaped in 27 ears (4.5%) which not confirming the findings of our study.(Kobayashi)

Using a surgical microscope, 12 cerebellopontine angles were dissected from adult cadavers from both genders and measured with a caliper. Their mean area was 139.09 mm² (86.45- 196.04 mm²) (Barreto). This value is much higher than the values found in this study, which were 41.9 mm² Fujita and Sando used a software to measure the length and the distance between the canal and vestibular aqueduct in 10 temporal bones of cadavers aged 4 months to 70 years and found that the length ranged from 5.9 to 11.7 mm and the distance ranged from 6.2 to 12 mm. They also measured the length and AP diameter in 108 temporal bones of adults of both genders and found them to be 11.5 mm and 3.6 mm, respectively .(Silverstein)

In 242 samples from individuals aged 16 to 93 years, the opening width was 4.5 mm (3-7 mm), the AP diameter was 4.6 mm (2-7 mm) and the length was 9.2 mm (6-14 mm). The same author using the same sample found AP diameters from 4. 0 to 5.0 and lengths from 8.0 to 11 (21-22). In mm mm mm 108 temporal bones, the AP diameter was 4 mm (2-6 mm) and the length was 8.5 mm (5-14 mm) (Moran).

Using the same methodology in temporal bones separated by gender, Lang found a length of 11.15 mm, an AP diameter ranging from 3.0 to 7.0 mm, and an opening width of 6.46 mm. In children, Lang reported a 7.23 mm length, a 4.6 mm AP diameter and

a 4.3 mm opening width. Our study found a slightly greater area and opening width in children.

A Sergio Ricardo study found there are no statistical differences between the areas, external opening widths and distances between the IAC and vestibular aqueducts between children and adults of both genders. However, there are statistical differences between its length in adults and children and its AP diameter. In this study we found there is no significant difference between opening width, length of canal, AP diameter and areas between children and adult of both genders .however, there are statistical differences between its distance of IAC /VA in adult and children.

5.2conclusion

1. Normal internal auditory canal shape varies greatly.
2. There are no statistical differences between the opening width, length of canal ,AP diameter and areas between children and adult of both genders .However , there are statistical differences between its distance of IAC /VA in adult and children.
3. There is no significant differences were detected between the normal right and left IAC measerments.
4. There is no significant difference in measurements in different gender except for AP diameter.
5. Measurement of the IAC length, opening width, AP diameters, area and the distance between IAC and VA can be important to surgical planning and interventional examination.
6. CT is considered as excellent method to determine normal internal auditory canal diameters and its shape.
7. A thorough knowledge of the normal anatomy of the temporal bone and the anomalies that affect it are important for interpreting radiographs, as it improves the quality of the results and allows development of a new diagnostic criterion.

5.3 Recommendation

1. Further studies of the IAC normal dimensions in specific age groups using HRCT is recommended.
2. Further studies of the IAC dimensions in pathological people and the affected of the pathology to the canal is recommended.
3. The Study IAC dimensions and its correlation to audiometric tatus and cerebropontine angle changes is recommended to determine other significant physiologic correlations.
4. Further study about the use of HRCT compare to MRI in assessment of IAC anatomy recommended.
5. Further studies of the IAC dimensions with increase number of samples size in different Sudanese tribe using HRCT is recommended.

References:

1. Agirdir BV, Sindel M, Arslan G, Yildirim FB, Balkan EI, Dinç O (2001) The canal of the posterior ampullar nerve: an important anatomic landmark in the posterior fossa transmeatal approach. *Surg Radiol Anat*, 23: 331–334.
2. Agur, A.M.R., Dalley, A.F., 2013. Cranial nerves. In: Grant's atlas of anatomy, 13th ed. Wolters Kluwer/Lippincott Williams & Wilkins, Philadelphia, pp. 817–850.
3. Alan. The essential guide to image processing. Academic press. pp, (2004). 743-9. .(mri basic principle and applicactin brain m dalemark a brown rechar d c5 editin 2015publisher jonh wiley 1
4. Barreto EC, de Carvalho GA. [Microanatomy of the cerebellopontine angle with morphometric analysis of the internal acoustic meatus]. *Arq Neuropsiquiatr*. 1993;51(2):213-6.
5. Bathla, G., Hegde, A.N., 2013. The trigeminal nerve: An illustrated review of its imaging anatomy and pathology. *Clinical Radiology* 68, 203–213.
6. Becker, M., Kohler, R., Vargas, M.I., Viallon, M., Delavelle, J., 2008. Pathology of the trigeminal nerve. *Neuroimaging Clinics of North America* 18, 283–307.
7. Belluscio, L., Lodovichi, C., Feinstein, P., Mombaerts, P., Katz, L.C., 2002. Odorant receptors instruct functional circuitry in the mouse olfactory bulb. *Nature* 419, 296–300.
8. Binder, D.K., Sonne, C., Fisschbeln, N.J., 2010. Cranial nerves: Anatomy, pathology, imaging. Thieme Medical Publishers, New York. Borges, A., Casselman, J., 2007. Imaging the cranial nerves: Part I: Methodology, infectious and inflammatory, traumatic and congenital lesions. *European Radiology* 17, 2112–2125.
9. Brazis, P.W., Lee, A.G., 1998. Binocular vertical diplopia. *Mayo Clinic Proceedings* 73, 55–66.
10. Brunsteins DB, Ferreri AJ (1995) Microsurgical anatomy of arteries related to the internal acoustic meatus. *Acta Anat (Basel)*, 152: 143–150.
11. Burchiel, K.J., 2011. Glossopharyngeal neuralgia. *Journal of Neurosurgery* 115, 934–935, author reply 935.
12. Capó, H., Warren, F., Kupersmith, M.J., 1992. Evolution of oculomotor nerve palsies. *Journal of Clinical Neuro-Ophthalmology* 12, 21–25.
13. Carroll, E.W., Wong-Riley, M.T., 1984. Quantitative light and electron microscopic analysis of cytochrome oxidase-rich zones in the striate cortex of the squirrel monkey. *The Journal of Comparative Neurology* 222, 1–17.
14. Chakeres DW. CT of ear structures: a tailored approach. *Radiol Clin North Am*. 1984;22(1):3-14.
15. Dacey, D.M., 1996. Circuitry for color coding in the primate retina. *Proceedings of the National Academy of Sciences of the United States of America* 93, 582–588.
16. Dekeyser, S., Lemmerling, M., 2009. MRI of abducens nerve paralysis of non-traumatic origin. *JBR-BTR* 92, 296–298.

17. Della-Morte, D., Rundek, T., 2012. Dizziness and vertigo. *Frontiers of Neurology and Neuroscience* 30, 22–25.
18. Driscoll CLW, Jackler RK, Pitts LH, Banthia V (2000) Is the entire fundus of the internal auditory canal visible during the middle fossa approach for acoustic neuroma? *Am J Otol*, 21: 382–388.
19. Dulguerov, P., Allal, A.S., Calcaterra, T.C., 2001. Esthesioneuroblastoma: A meta-analysis and review. *The Lancet Oncology* 2, 683–690.
20. Farahani RM, Nooranipour M, Nikakhtar KV (2007) Anthropometry of internal acoustic meatus. *Int J Morphol*, 25: 861–865.
21. Fatterpekar GM, Mukherji SK, Lin Y, Alley JG, Stone JA, Castillo M (1999) Normal canals at the fundus of the internal auditory canal: CT evaluation. *J Comput Assist Tomogr*, 23: 776–780
22. Fujita S, Sando I. Postnatal development of the vestibular aque duct in relation to the internal auditory canal. Computer-aided three-dimensional reconstruction and measurement study. *Ann Otol Rhinol Laryngol*. 1994;103(9):719-22.
23. Gray, Henry, Carter, Henry Vandyke (1858) *Anatomy Descriptive and Surgical*, London: John W. Parker and Son, retrieved 16 October 2011
- GUIRADO R. C. [Malformations du conduit auditif interne. Bordeaux, FRANCE: *Revue de laryngologie, otologie, rhinologie*]; 1992.
24. Hallowell, Davis and S. Richard Silverman (ED), 1970. *Hearing and Deafness*, 3rd ed., Holt, Rinehart and Winston.
25. Lorrie L K, Connie M P, Sectional anatomy for imaging professionals. 2^{ed} edition. United States: Mosby, 2007.
26. Stephanie Ryan Michele McNicholas Stephen Eustace 2004 25 28 *Anatomy for Diagnostic Imaging* second edition The publisher's policy is to use paper manufactured from sustainable forests
27. Merchant and Nobel 2010 schematic of circulation of inner ear, from Schuklencht, S. Pathology of the ear Patriani AF, Braga FM. Estudo do meato acústico interno e do ângulo pontocerebelar com a tomografia axial computadorizada associada a cisternografia com ar. 1987;6(1).
28. Paparella MM, Shumrick DA, Gluckman JL, Meyerhoff WL. *Otolaryngology: Basic Sciences and Related Principles*. Philadelphia: Saunders; 1991.
29. Pellet W, Cannoni M, Pech A, Jacomy JP. *Otoneurosurgery*. Germany: Springer; 1990.
30. Valvassori GE, Pierce RH. The Normal Internal Auditory Canal. *Am J Roentgenol Radium Ther Nucl Med*. 1964;92:1232-41.
31. Vilain J, Pigeolet Y, Casselman JW. Narrow and vacant internal auditory canal. *Acta Otorhinolaryngol Belg*. 1999;53(1):67-71.
32. Virapongse C, Rothman SL, Kier EL, Sarwar M. Computed tomographic anatomy of the temporal bone. *AJR Am J Roentgenol*. 1982;139(4):739-49
33. Kobayashi H, Zusho H. Measurements of internal auditory meatus by polytomography. 1. Normal subjects. *Br J Radiol*. 1987;60(711):209-14

- 34.Barreto EC, de Carvalho GA. [Microanatomy of the cerebellopontine angle with morphometric analysis of the internal acoustic meatus]. *Arq Neuropsiquiatr*. 1993;51(2):213-6.
- 35.Silverstein H, Norrell H, Smouha E, Haberkamp T. The singular canal: a valuable landmark in surgery of the internal auditory canal. *Otolaryngol Head Neck Surg*. 1988;98(2):138-43.
- 36.Moran C. [Anatomy of the internal auditory canal]. *Rev Laryngol Otol Rhinol (Bord)*. 1972;93(11):727-36.
- 37.Lang J. Clinical anatomy of the cerebellopontine angle and internal acoustic meatus. *Adv Otorhinolaryngol*. 1984;34:8-24.
- 38.Sergio Ricardo Marques 1*, Sergio Ajzen 2, Giuseppe D'Ippolito 2, Luis Alonso 1, Sadao Isotani 3, Henrique Lederman 2. Iran J Radiol. 2012;9(2):71-78. DOI: 10.5812/iranradiol.7849.
- Morphometric Analysis of the Internal Auditory Canal by Computed Tomography Imaging
- 39Moran C. [Anatomy of the internal auditory canal]. *Rev Laryngol Otol Rhinol (Bord)*. 1972;93(11):727-36.

Appendix I

Data collection sheet

	Gender	Age	Opening width	Length	Area of canal	Shape of canal	Diameter between IAC/VA
Rt IAC							
Lf IAC							